



NEURAL DYNAMICS IN CORTEX–STRIATUM CO-CULTURES—II. SPATIOTEMPORAL CHARACTERISTICS OF NEURONAL ACTIVITY

D. PLENZ*† and A. AERTSEN‡

†Max-Planck-Institut für biologische Kybernetik, Spemannstrasse 38, 72076 Tübingen, Germany

‡Center for Research of Higher Brain Functions, Department of Neurobiology, Weizmann Institute of Science, Rehovot 76100, Israel

Abstract—Neural dynamics in organotypic cortex–striatum co-cultures grown for three to six weeks under conditions of dopamine deficiency are described. Single neuron activities were recorded intra- and extracellularly, and spatiotemporal spreading of population activity was mapped using voltage-sensitive dyes. The temporal properties of spike firing were characterized by interspike interval histograms, autocorrelation and crosscorrelation.

Cortical pyramidal neurons ($n = 40$) showed irregular firing with a weak tendency to burst or to oscillate. Crosscorrelations revealed strong near-coincident firing and synaptic interactions. Disinhibition was a notable feature in a strongly firing cortical interneuron. Cortical activity spread in the co-culture, thus inducing an overall, homogeneous depolarization in the striatal part. Striatal cells were divided into principal cells and type I and II secondary cells. Principal cells ($n = 40$) were similar to those reported previously *in vivo*. Spiking activity ranged from irregular spiking at very low rates to episodic bursting, with an average burst duration of 1 s. Interspike intervals were single-peaked. Intracellular recordings revealed characteristic, long-lasting subthreshold depolarizations (“enabled state”) that were shortened by local muscarinic receptor blockade. During prolonged time periods in the “enabled state”, locally applied bicuculline induced strong firing in most principal neurons. Striatal secondary type I neurons ($n = 25$) showed high spiking rates, single- and double-peaked interval histograms and low-threshold, short-lasting stereotyped bursting activity and occasional rhythmic bursting. The firing of these neurons was increased by bicuculline. Crosscorrelations showed synchronization of these cells with principal cell activity. Secondary type II neurons ($n = 15$) revealed tonic, irregular firing patterns similar to cortical neurons, except with occasional firing in doublet spikes.

We conclude that under conditions of dopamine deficiency in corticostriatal co-cultures (i) the cortex induces the “enabled” state and typical bursting mode in striatal principal neurons; (ii) principal neurons are strongly inhibited during the “enabled” state; (iii) muscarinic activity, presumably from tonically active striatal cholinergic interneurons, stabilizes the “enabled” state; (iv) striatal GABAergic interneurons receive synaptic inhibition and take part in synchronized activity among striatal principal cells. Our results favor the view of the striatum as a lateral inhibition network.

Key words: neural network, system analysis, pyramidal neuron, medium-spiny projection neuron, interneuron, crosscorrelation.

A key element to understand cortex–basal ganglia interactions resides in the neural activity pattern elicited in the striatum by cortical input. Most cortical areas project to the striatum⁸⁵ and the main striatal target of cortical activity is the GABAergic,^{69,71,97,111} medium-sized, spiny^{21,136,141} projection^{29,89,105,120} neuron (principal neuron), which accounts for more than 90% of striatal neurons.^{63,82,118} As the axons of these neurons, besides having local axon collaterals,^{15,17,62,105,141} immediately

leave the nucleus, the striatum functionally behaves as a “sheet”: it can be regarded as a one-layered, locally operating neural network, with only one synapse between the input and the output.^{104,133,134} The anatomical picture strongly favors the view of the striatum as a lateral inhibition network.^{15,17,105,141} Surprisingly, however, direct electrophysiological evidence for this view is remarkably weak.^{59,61,80,98,110}

The information extracted by the striatum from cortical input activity is not known. In contrast to cortical neurons, striatal principal neurons fire in episodic bursts.² In a number of studies dealing with striatal activity during movement in rats^{46,102,129,132} and monkeys,^{3,20,38,56,58,65,66,93,95,117} it was shown that these bursts strongly relate to external actions, such as movement on the part of the animal. From intracellular recordings *in vivo* it is known that bursts occur

*To whom correspondence should be addressed at: University of Tennessee, Department of Anatomy and Neurobiology, College of Medicine, 875 Monroe Avenue, Memphis, TN 38163, U.S.A.

Abbreviations: AC, first order autocorrelation of spike/unit activity; AHP, afterhyperpolarization; CC, first order crosscorrelation of unit activities.

only during a depolarized, subthreshold state.^{137,142} Furthermore, bursts in principal neurons are not the result of intrinsic, oscillating calcium potentials,^{25,70} but depend critically on cortical input.² Thus, it is likely that the occurrence of a burst in a striatal principal neuron indicates some significant feature of cortical activity. At present, two, mutually, non-exclusive views on burst activity in principal neurons dominate. From single-neuron studies *in vivo*^{34,75,139,142} and models of single-neuron dynamics,¹³⁶ principal neurons are viewed as coincidence detectors of corticostriatal inputs. In this view, the time of occurrence of a burst is governed by intrinsic membrane dynamics.¹³⁷ In contrast, theoretical studies focusing on interactions among striatal neurons have stressed the emergence of principal neuron bursts as a result of mutual inhibition in the striatal network.^{4,133,134}

When considering striatal dynamics, at least two additional types of striatal neurons are of importance. The first type are the striatal GABAergic interneurons, which also receive cortical input.^{69,77,112} Anatomical findings indicate that these interneurons most probably take part in strongly inhibitory, local striatal loops.^{18,28,69,71,72} These neurons seem to fire in high-frequency bursts upon cortical stimulation.^{69,112,135} The second type is characterized by its regular, tonic activity pattern.^{2,7,68} In the monkey, tonically active neurons are much more strongly related to external, set-dependent⁶⁸ and reinforcing⁹ events than to the generation of movement events. Cholinergic striatal interneurons might constitute at least part of this population of tonically active neurons,^{8,140} giving rise to a continuous cholinergic influence on striatal network dynamics.

Here, we have studied cortex–striatum interactions using a new organotypic co-culture system described in the companion paper.^{104a} The benefits of adopting this approach are three-fold. Firstly, the information conveyed by burst activity in principal neurons may be more easily analysed in an “open loop” system, in which an isolated striatal network is driven by activity from a cortical network (a similar approach has recently been used in a modeling study^{133,134}). An important issue is the question of to what extent striatal principal cell activity in such a system exhibits similar dynamics as those observed *in vivo*, given a cortical network dynamics with at least a minimum of correlated activity. An answer to this question will help to dissect some of the main modes of corticostriatal interactions. Secondly, to examine the cholinergic contribution to principle neuron dynamics, an appropriate experimental preparation, i.e. one which preserves the cholinergic interneuron activities, is of prime importance. Finally, a classification of the firing patterns of GABAergic interneurons and their relationship to striatal dynamics will contribute substantially to our understanding of striatal processing. We will demonstrate that the organotypic cortex–striatum co-cultures present an adequate *in vitro* system to study these issues, and describe the funda-

mental neural dynamics that emerge from the corticostriatal interactions.

EXPERIMENTAL PROCEDURES

Preparation of organotypic cortex–striatum co-cultures

A detailed description is given in the companion paper.^{104a} In brief, the brains of newborn Sprague–Dawley rats (postnatal days 0–2; colony maintained at MPI für Virusforschung, Tübingen) were sliced transversely (350 μm) on a Vibratome (Campden). For further dissection only slices comparable to coordinates bregma 1.7 to –1.3 for adult rat brains⁹⁹ were used. Single tissue pieces from somatosensory and motor cortex (dorsal or dorsolateral^{155,131}) and caudate–putamen (dorsal or dorsolateral) were dissected under stereomicroscopic observation. Tissue pieces were placed on a membrane (Millicell-CM, Millipore PICM) on a coverslip with the striatal tissue always close to the white matter. For comparative studies single striatal cultures from the same regions as described above were prepared. Single cultures and co-cultures were embedded and grown according to the roller tube technique^{44,45} for three to six weeks. No dopamine was added.

Recording conditions

Co-cultures were submerged in a recording chamber (total volume *c.* 500 μm). Saturated (95% O₂, 5% CO₂) Hank's balanced salt solution (Gibco) with 2 mM CaCl₂ added was used as extracellular medium. The extracellular concentrations of potassium ([K⁺]_o), hydrogen carbonate ([HCO₃⁻]_o) and calcium ([Ca²⁺]_o) were estimated to be 5.8, 4.8 and 2.9 mM, respectively (see Ref. 116). The flow rate was set to 2–3 ml/min and the temperature was held at 35 \pm 1°C. The recordings were started after the co-cultures had been left in the new environment for 30–60 min. During the experiment the total number of swollen cell bodies could increase. However, very often recordings were done for up to 10 h from a single co-culture without any signs of electrophysiological deterioration. The glass chamber bottom allowed for visual selection of cells and for additional optophysiological recordings.

Stimulation

A tungsten electrode (0.005 in., Phymep) connected to a stimulus isolator unit (WPI, A 360; stimulus pulse: 20–200 μA , 50 μs ; interstimulus interval: 5–30 s) was placed under visual control in the lower third of the cortical tissue (layers V/VI).

Intracellular recording

Intracellular recordings were obtained with sharp microelectrodes (90–140 M Ω) containing 2 M potassium acetate and 2% neurobiotin (Vector). Striatal interneurons were visually selected according to their large cell body. The majority of cells with a diameter below 20 μm were considered to be striatal principal cells (see companion paper). Stable intracellular recordings ranged from 10 min to several hours. Cells were accepted if they showed (i) an action potential maximum of at least 0 mV, (ii) a stable resting membrane potential and (iii) no cell body swelling. Signals were recorded with conventional electronics made in our institute. Intracellular electrophysiological signals were filtered between 0 and 1 kHz (80 dB/decade), digitized (10–20 kHz) and analysed on a PC (Spike2 4.0, Cambridge Electronic Design). Multiple resolution spike interval histograms and first order autocorrelations of spike/unit activity (ACs) were calculated for each cell using bin widths ranging from 1 to 16 ms.

Extracellular recording

Extracellular recordings, lasting for several hours, were done with glass microelectrodes (3–9 M Ω) containing 3 M

NaCl. Signals were recorded with conventional electronics made in our institute, filtered [0–1(3) kHz; 80 dB/decade] and digitized on a PC (10–33 kHz; Spike2 4.0, Cambridge Electronic Design). Because of the low sample rate in experiments involving multiple channels (12 kHz/channel), no classification of extracellular spike forms was done. Units were detected either on-line using a template (minimum number of events: 8; maximum amplitude variance: 20%; d.c. correction on), or off-line using a simple threshold mode to detect the rising or falling phase of a spike. The minimum interval between adjacent events in the off-line mode was set to 1–3 ms. When using template matching, all units crossing threshold but not matching the template(s) were also stored, thus allowing the off-line checking of appropriate sampling. Spike interval and post-stimulus time histograms, ACs and first order crosscorrelations of unit activities (CCs) were calculated using bin widths from 1 to 16 ms.^{100,101}

Optophysiology

For optical recording co-cultures were stained with the voltage-sensitive styryl dye RH237 (A. Grinwald, gift) by bath application for 15 min. The spatiotemporal distribution of relative fluorescence change (resolution: 150 × 150 μm, 0.5 ms) induced by local cortical microstimulation was recorded over trials of 96 ms (interstimulus interval: 30 s) using a 12 × 12 photodiode array (Zeiss IM 35; Zeiss BP 546, FT 580, LP 590; Leitz: × 25 NPL Fluotar; array: Centronics). The level of spontaneous activity was monitored by an extracellular microelectrode in the cortical or the striatal part of the co-culture and the cortex was stimulated during periods of low spontaneous activity. In order to cover the spatial extension of a co-culture (4–6 mm²), the photodiode array was shifted between several different locations on successive trials.¹⁰³ The partially overlapping fields were merged on the basis of their absolute coordinates. In the case of overlapping photodiode positions the mean was taken. The results of two to three stimuli were averaged at each location. Signals from the photodiode array were current–voltage converted and stored on a PDP11/73 (Digital; for details see Bonhoeffer and Staiger¹⁹ and Plenz and Aertsen¹⁰³). For each photodiode location and for each time sample the relative fluorescence change was calculated on a VAX-750 (DEC). The relative fluorescence change was obtained by subtracting the absolute fluorescence without stimulus from the fluorescence with stimulus, and by subsequently dividing this difference by the absolute fluorescence measured.^{33,49,50,115} This relative fluorescence change matches the intracellular membrane potential change at the single-cell level¹⁹ and is in accordance with field potential measurements and current source density profiles of the population activity.¹⁰³ Further processing and graphical display were done on a SPARC-station IPX (SUN) using the IDL software (Interactive Data Language, version 2.2, Research Systems).

Drug application

(–)-Bicuculline methiodide (0.07 M; Sigma B6889) or atropine sulfate (0.01 M; Research Biochemicals Inc. A-105) were dissolved in artificial cerebrospinal fluid and were locally pressure microejected (10–70 kPa; 0.2–2 s; Neuro Phore BH-2; Medical System Corporation) with a single glass microelectrode. The tip of the electrode was broken to a diameter of 2–3 μm and was placed under microscopic control in the vicinity of the recorded cell. To ensure a highly localized drug application, the application electrode was in most cases lowered after penetration was established. To minimize drug diffusion from striatum to cortex, the flow was adjusted from the cortex to the striatum. The locality of drug application was additionally checked by monitoring the activity at distant locations or by repeating the drug application at locations distant from the recorded cell.

RESULTS

Spontaneous activity was measured in more than 100 cortex–striatum co-cultures cultured for three to six weeks. We recorded intracellularly from 94 neurons (see companion paper Ref. 104a). From this set, 54 neurons were used for statistical analysis of spike timing properties. A further 66 extracellular recordings were analysed with the same techniques.

Cortical pyramidal cells

Spontaneous cortical activity was characterized by periods of low activity interrupted by high activity periods (Figs 1A, 2A). During high activity periods the membrane potential showed large numbers of spontaneous, presumably synaptic potentials (Figs 1B, 2B) and average discharge was three to four spikes per second (Table 1). Pyramidal cells were grouped according to their AC, which either revealed a decrease ($n = 5$) or an increase ($n = 12$) in spike discharge during the first 100 ms following an action potential. Both types of ACs were found throughout all cortical layers. An example of a pyramidal cell showing a decrease in spike discharge during the first 70 ms is shown in Fig. 1F. In these cells spike interval histograms had a single peak with a modal interval in the range of 130 ms (Fig. 1C, E; Table 1). Cells showing an increase in spike discharge (cf. Fig. 2F) had spike interval histograms which occupied a broad range of interspike intervals. An early peak around 10–20 ms followed in most cases (10 of 12) by a substantially weaker, very broad second peak at 100–200 ms was revealed (Fig. 2C, E; Table 1). The tendency to burst was weak: only a small fraction of spikes fell within interspike intervals below 30 ms (e.g. Fig. 2F). On a time scale of 1–2 s ACs of both types were flat.

Extracellular recordings were analysed from 20 cortical neurons (Fig. 3). During extracellular recordings we also measured activity triggered by local electrical microstimulation of the cortex (Fig. 3B; see also below). Maximal spike discharges, types of spike interval histograms and ACs were similar to those observed in intracellular recordings (Fig. 3, Table 1). In four cells a tendency to recurrent firing at 6.1 ± 2.5 Hz was found, as judged by an additional peak in the ACs after the initial spiking decrease (Figs 3D, 5D).

Crosscorrelation functions for spontaneous activity were calculated for 11 pairs of simultaneously recorded neurons. Multi-unit activity was recorded either from one or two electrodes. A tightly structured timing pattern was composed of strong near-coincident firing (eight of 11) and/or strong asymmetric correlation (five of 11; Fig. 4). Spontaneous activities from different units were recorded from two electrodes in the upper cortical region, 0.8 mm apart from each other. Unit activity on both electrodes showed alternating periods of high and low activity (Fig. 4A; dot displays). Single-unit activity on electrode 1 was selected by template matching. Multi-unit

P activity on electrode 2 was selected using a threshold for negative peaks. Single-unit activity on electrode 1 with multi-unit activity on electrode 2 was crosscorrelated. The CC on a large time scale clearly revealed a central peak, pointing to near-coincident firing (Fig. 4B). With higher time resolution this central peak was composed of a narrow, near-coincident peak and a considerably broader peak, both situated asymmetrically with respect to the

origin (Fig. 4C). Thus, units on electrode 2 fire in near-coincident fashion with unit 1 (from simultaneous to within a 5 ms delay), and/or with a larger delay (within the next 20 ms) after a spike in unit 1 had occurred. These findings point to strongly correlated activity among cortical neurons in the culture system.

Similar CCs were found during periods of increased activity, lasting up to several seconds, evoked

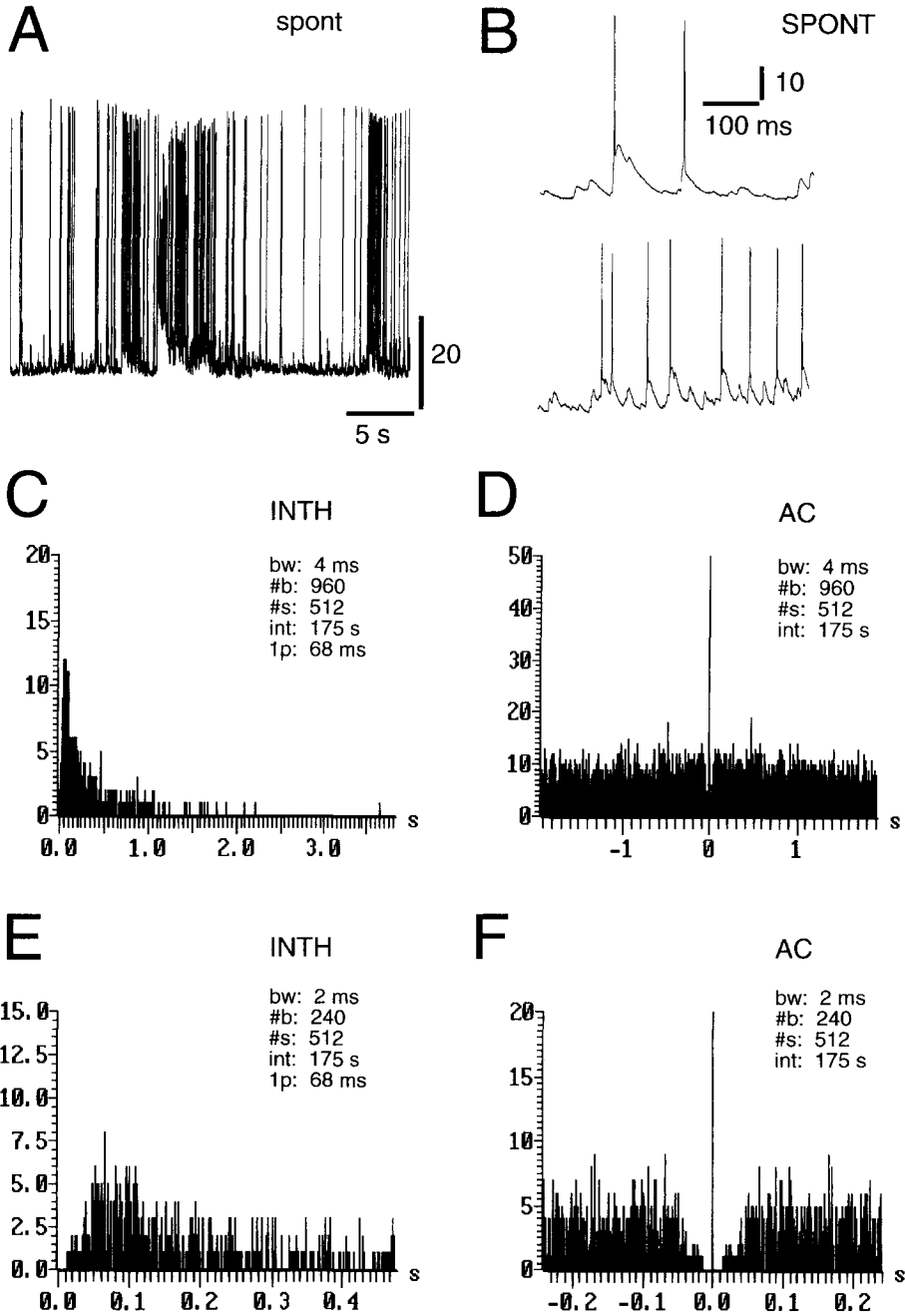


Fig. 1. Spontaneous activity (spont) in pyramidal cells with no tendency to burst. (A) Intracellular recording with high and low activity periods. (B) Magnified view of intracellular time course during low (upper) and high (lower) activity periods. (C, E) Single-peaked spike interval histograms (INTHs) of the neuron shown in A with a modal spike interval of 68 ms. (D, F) Flat ACs of spiking activity with a decrease in spike discharge during the first 70 ms.

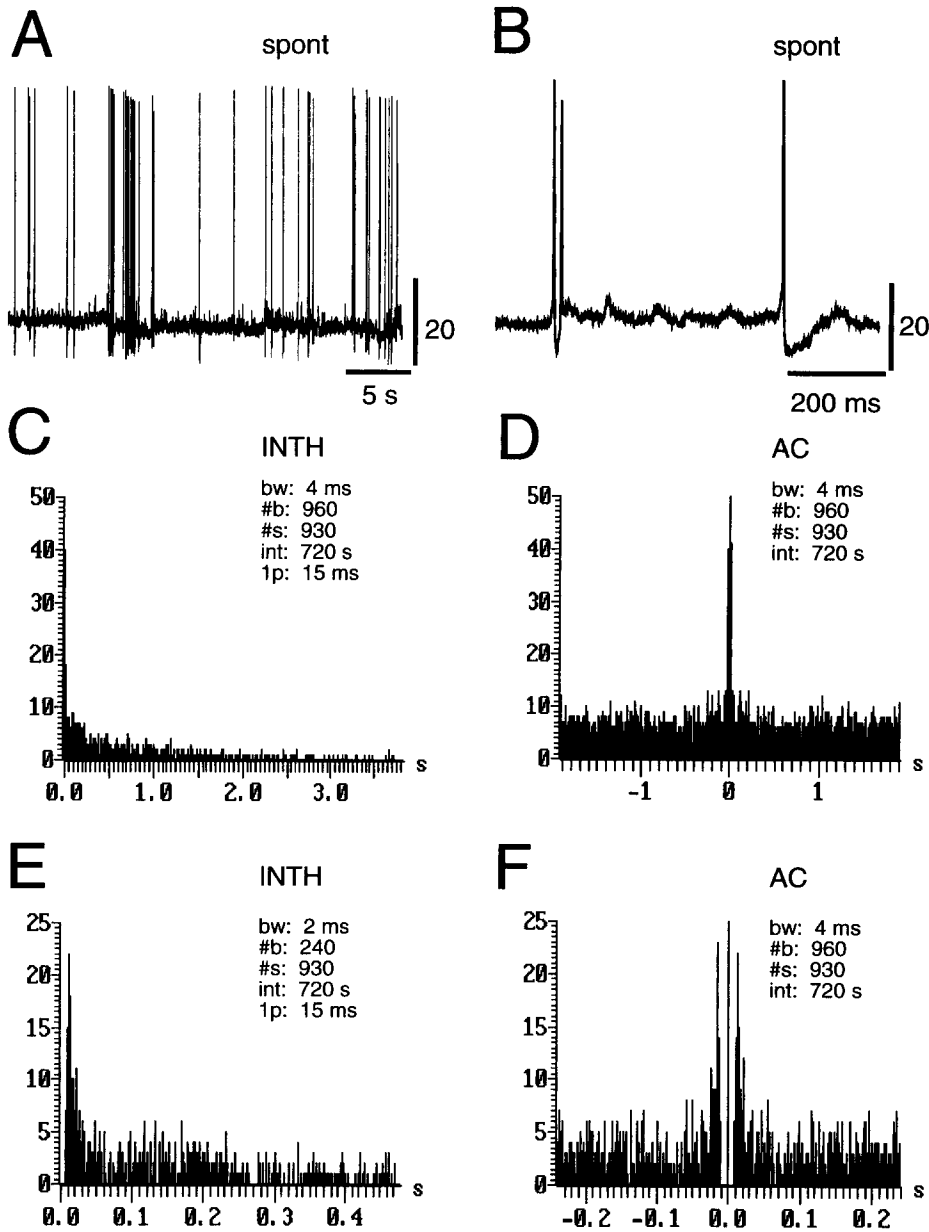


Fig. 2. Spontaneous activity in pyramidal cells with tendency to burst. (A) Intracellular recording with low and high activity periods. (B) Magnified view of intracellular time course shows the occurrence of short spike intervals. (C, E) Spike interval histogram of the neuron shown in A. The broad distribution reveals an increase of spike intervals around 15 ms. (D, F) The AC is flat, except for an increase in spike discharge during the first 30 ms after a spike.

by cortical microstimulation ($n = 6$; Fig. 5). In most cases a cortical unit fired one to several spikes within a few milliseconds after stimulation. These early spikes were followed by a period of spike depression, with a subsequent long-lasting spike discharge. The maximum discharge during the long-lasting excitation occurred about 1 s after stimulation (Fig. 5A, B, Table 1). The early spikes generally escaped the template sampling because of underlying field potential shifts; these shifts were particularly strong during the first milliseconds after stimulation.

No attempt was made to include these early discharges, since we were mainly interested in the steady-state the cortical dynamics achieved after stimulation. The CCs revealed prominent near-coincident peaks (Fig. 5E), which under high time resolution (Fig. 5F) were actually asymmetric about the origin, indicating that the units fired sequentially. Thus, local cortical microstimulation triggered a long-lasting activity increase, during which cortical neurons showed stable, strongly correlated activity.

Cortical interneurons

The spontaneous intracellular activity of the cortical interneuron (see Ref. 104a) was characterized by periods of strong depolarization, with three to four times higher spiking activity than in cortical pyramidal cells (Table 1). High activity periods alternated with periods without any visible activity. The membrane potential time course after an activity period was characterized by a slow decay (Fig. 6A, arrow). Spikes had prominent afterhyperpolarizations (AHPs) (Fig. 6B) and although short interspike intervals were present, the majority of spikes were followed by 40–80 ms of spike depression (cf. Fig. 6D, F with Figs 1 and 5). The spike interval histogram showed several peaks and the AC revealed a tendency to oscillate at 8–9 Hz.

A tendency to oscillate might result from the local network dynamics, as cortical interneurons are involved in an inhibitory feedback circuit with cortical pyramidal cells, which can lead to oscillations depending on the balance between time delays and gain. We tested whether the oscillations result from a strong excitatory drive in that feedback loop by local application of the glutamatergic antagonist 6-cyano-7-nitroquinoxaline-2,3-dione (1 s; 25 kPa) and recording the ongoing spiking activity for 190 s. Under these conditions the oscillations disappeared (Fig. 6F); however, the firing frequency was almost tripled during high activity periods. This points to strong disinhibition among cortical interneurons (see Discussion). Nevertheless, the inhibition present in the cortex was large: removal of inhibition by applying the GABA_A antagonist bicuculline led to an immediate and strong depolarization of cortical

neurons, accompanied by spike blockade, burst discharge and profound burst AHP ($n = 4$; Fig. 7) reminiscent of epileptic discharge in the neocortex.^{51,54,74,78}

Spatiotemporal activity dynamics revealed by optophysiology

The presence of corticostriatal projection neurons in the co-cultures was confirmed anatomically in the companion paper. Here we show that (i) the cortical culture can actually “drive” the striatal network and (ii) the spatiotemporal characteristics of the activity are produced by cortical excitation. From the extracellular recordings it was evident that cortical microstimulation induced a period of increased activity lasting up to several seconds in the cortical and striatal parts of the co-culture (see Figs 3B, 5, 12, 15 and poststimulus time histogram in Tables 1–4). This activity was synaptically mediated, since it was blocked under low calcium/high magnesium conditions ($n = 3$).

Using optophysiology with voltage-sensitive dyes we could show that in all cases ($n = 8$) the induced spread of activity in the co-culture system was basically the same: local electrical microstimulation in the cortex induced a depolarization propagating in the cortical culture (Fig. 8). After a latency of 8–13 ms, an activity wave spread through the entire striatal tissue. In all cases this spatiotemporal pattern of striatal activation had an overall depolarizing effect. No striatal regions with net hyperpolarization were found. After approximately 20 ms a stable pattern of homogeneous depolarization was reached, which lasted for at least a further 75 ms (i.e. until the end

Table 1. Spiking activity of cortical neurons in cortex–striatum co-cultures

	Intracellular	<i>n</i>	Extracellular	<i>n</i>
Age (days)	24 ± 4	17	28 ± 3	20
Fmax† (spikes/s)*	3.4 ± 0.9	17	3.8 ± 2.9	20
Δt‡ (ms)*	113 ± 59	5	104 ± 75	9
INTH§ (ms)*	152 ± 51	5	130 ± 90	9
INTH 1p (ms)*	14 ± 6	12	11 ± 9	11
INTH 2p¶ (ms)*	131 ± 41	10	161 ± 32	7
PSTH exc**			979 ± 359	12

*Not different at $P < 0.05$; two-tailed Wilcoxon’s rank sum test.

†Maximum firing rate using a sliding integration window (integration width: 3 s) and taking peak value.

‡Total duration of decrease in spike discharge seen in the AC. Data taken from cortical neurons, which show a complete inhibition of spike discharge for at least 30 ms after a spike. Duration was defined as the time necessary to reach baseline activity after a spike discharge seen in the AC; this baseline level was estimated by visually applying a horizontal linear fit.

§Interval at maximum peak in the spike interval histogram (INTH). Same population of cortical neurons as in ‡.

||Interval at first peak in the spike interval histograms showing a bi-modal distribution of spike intervals. Only cortical cells showing a tendency to fire in bursts were included.

¶Interval at second peak in the spike interval histograms showing a bi-modal distribution of spike intervals. Same population as in ||.

**Time of maximum discharge during the long-lasting excitation seen in the poststimulus time histogram.

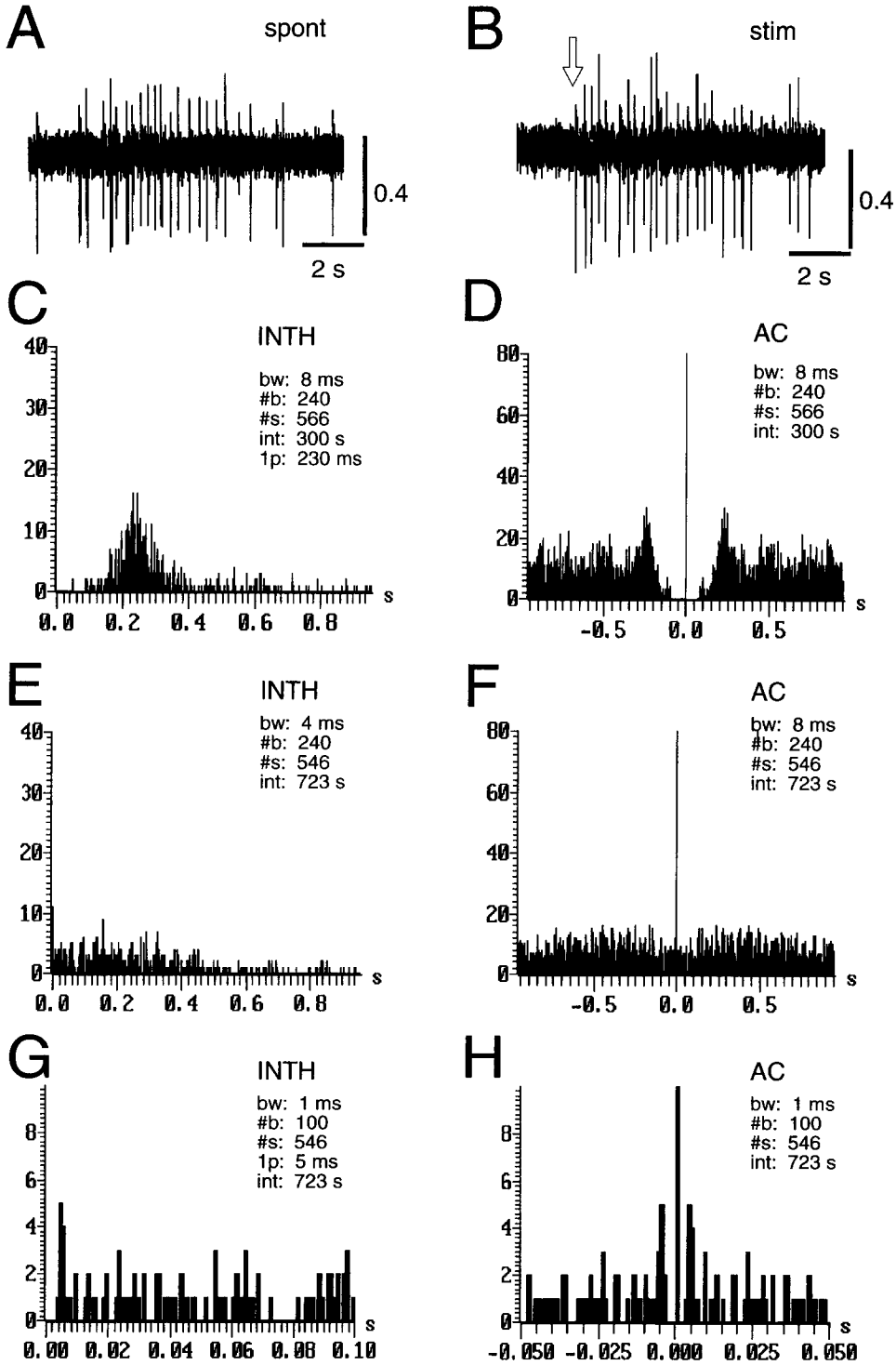


Fig. 3. Extracellular spiking activities from cortical cells. (A) Extracellular recording showing spontaneous (A) and stimulus evoked (B, arrow) spiking activity, mainly composed of one single unit. (C, D) Spike interval histogram and AC of the unit shown in A. The AC shows a strong decrease in spike discharge during the first 150 ms followed by a single short-lasting peak around 230 ms, indicating recurrent firing at 4–5 Hz. (E, G) Spike interval histogram of an extracellular unit showing a broad spike interval distribution, with an early peak at 5 ms. The AC (F, H) is flat, with a slight tendency to burst (5 ms); no strong depression in spike discharge can be seen.

of the recording trials). Further analysis of the spatio-temporal relative fluorescence change (color-coded surface plots, two-dimensional Fourier analysis) did not reveal any spatial periodicities or other signs of multiple centers of maximum depolarization in the striatal culture. The maximum amplitude of relative fluorescence change (e.g. 0.0065 in Fig. 8), estimated based on intracellular recordings (see Fig. 9), covered a range of *c.* 15 mV in the striatum. Due to a noise level of ± 0.001 , the sensitivity of the optical recordings was in the range of 4.6 mV. Thus we conclude that (i) activation of the cortical culture can actually drive the striatal network, (ii) cortical activation leads to an overall depolarization of the striatal tissue for

more than 75 ms, and (iii) during that time no net changes larger than *c.* 4.6 mV on a spatial scale of 150 μm occur at the population activity level.

The striatal neural dynamics described in the following section were never seen in single striatal cultures, i.e. without cortical tissue present ($n = 6$).

Striatal principal cells: intracellular recordings

The striatal principal cells represent the class of striatal medium-sized GABAergic projection neurons (see Ref. 104a).

The spontaneous membrane potential dynamics found in principal cells ($n = 34$) followed a characteristic time course: a subthreshold depolarization, with

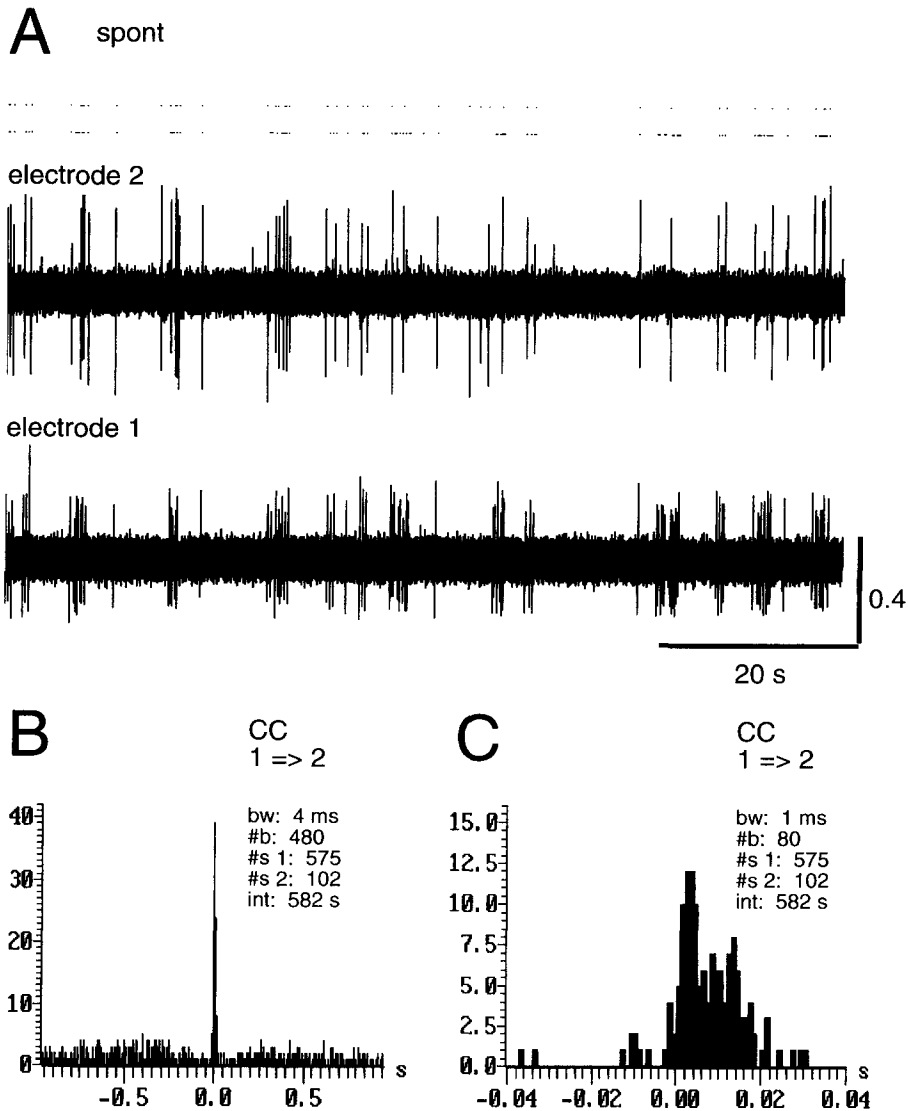


Fig. 4. CC of spontaneous cortical activity in cortex-striatum co-cultures. (A) Spontaneous extracellular single-unit activity from electrode 1 (time course and dot display; lower trace) and multi-unit activity from electrode 2 (time course and dot display; upper trace). The electrodes were placed 0.8 mm apart in the upper cortical layers. (B) CC from electrode 1 to units on electrode 2. A prominent central peak surrounded by weak depression is apparent. (C) Magnified view of CC in B. The central peak consists of near-coincident firing (up to 5 ms delay) and an additional, broader increase in firing probability for units on electrode 2, for around 20 ms after the unit on electrode 1 has fired.

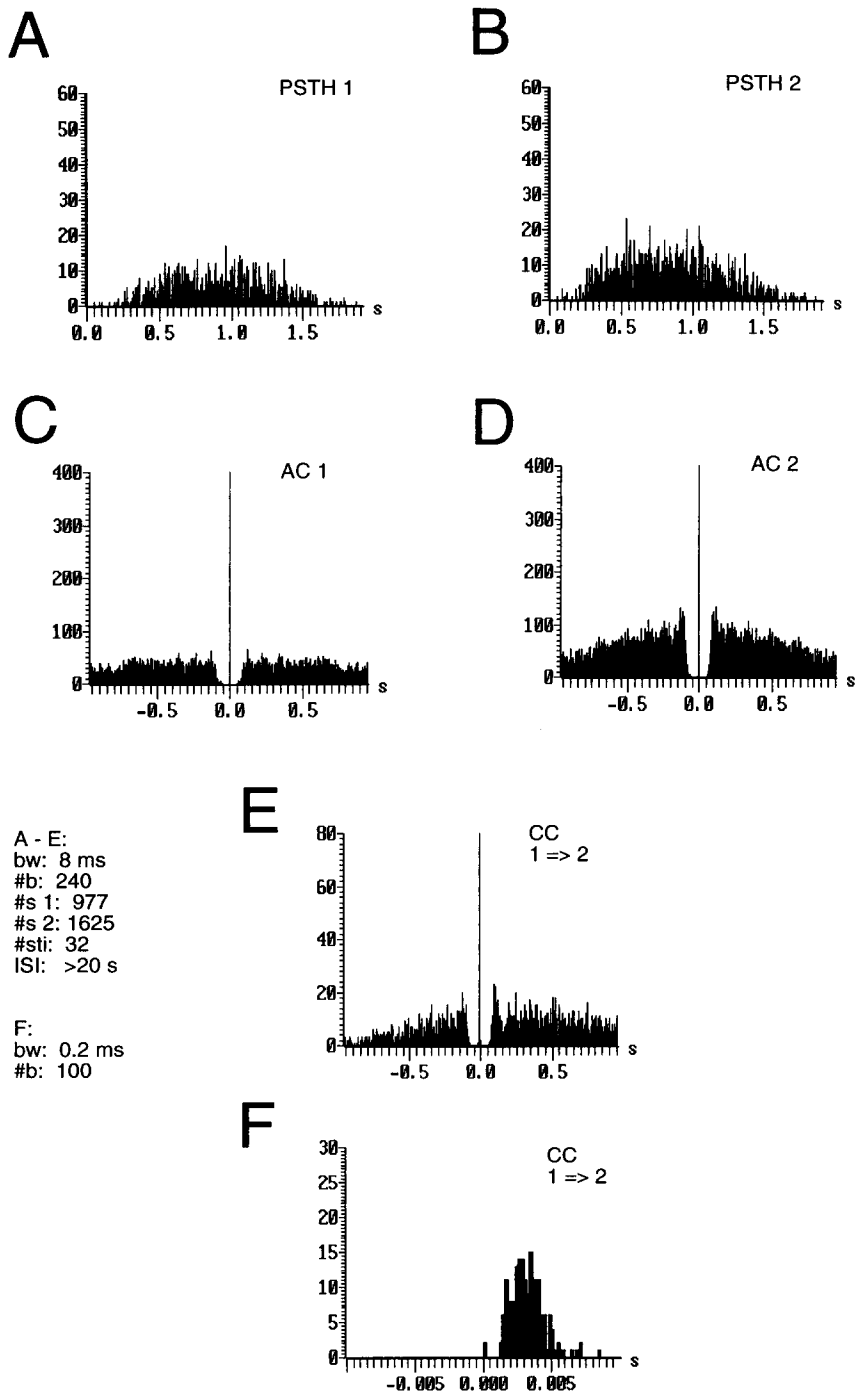


Fig. 5. CC of cortical activity evoked by cortical microstimulation. Units were sampled from one electrode using template matching. Poststimulus time histograms (A, B) and ACs (C, D) of units 1 and 2, respectively. (E, F) CC between units 1 and 2. Note the tight synchrony (< 6 ms) between these two evoked activities.

occasionally one single spike riding on it, was followed by a short-lasting stabilization in the subthreshold range before decaying to the resting potential (Fig. 9A). Upon long-lasting spontaneous depolarizations, this pattern was repeated with subsequent spiking activity (Fig. 9B, C). Prolonged periods of firing never occurred during the first

100 ms of depolarization onset. In 11 of 34 cells, spiking activity was high enough to calculate spike interval histograms and ACs. Maximal average firing rates were three to four spikes per second (Table 2) and spike interval histograms were always one-peaked (Fig. 9D, F: at 48 ms) with a modal interspike interval of 100 ms (Table 2). In each individual cell,

the mean interspike interval was much larger than the modal spike interval, and the average standard deviation was three times as large as the mean interval (Table 2). Thus, these neurons fired in bursts with an average burst duration of 1 s (Table 2). The statistical analyses from intracellular recordings were biased towards cells showing relatively high, i.e. bursting, activity. Often, principal cells showed very low firing rates, which were too low to be analysed (e.g. Figs 9A, 10C). Nevertheless, a characteristic common to all principal cells was the strong spike depression,

lasting for at least 20–30 ms after a spike (e.g. Fig. 9F; cf. with secondary neurons type I).

Striatal principal cells: “enabled state”

A striking pattern in the intracellular membrane potential dynamics of principal cells was the predominance of two distinct states, which was shown in the distributions of membrane potentials (Fig. 10A, B): one very polarized and one depolarized. Burst activity only occurred during the depolarized state, which was just a few millivolts below spike threshold.

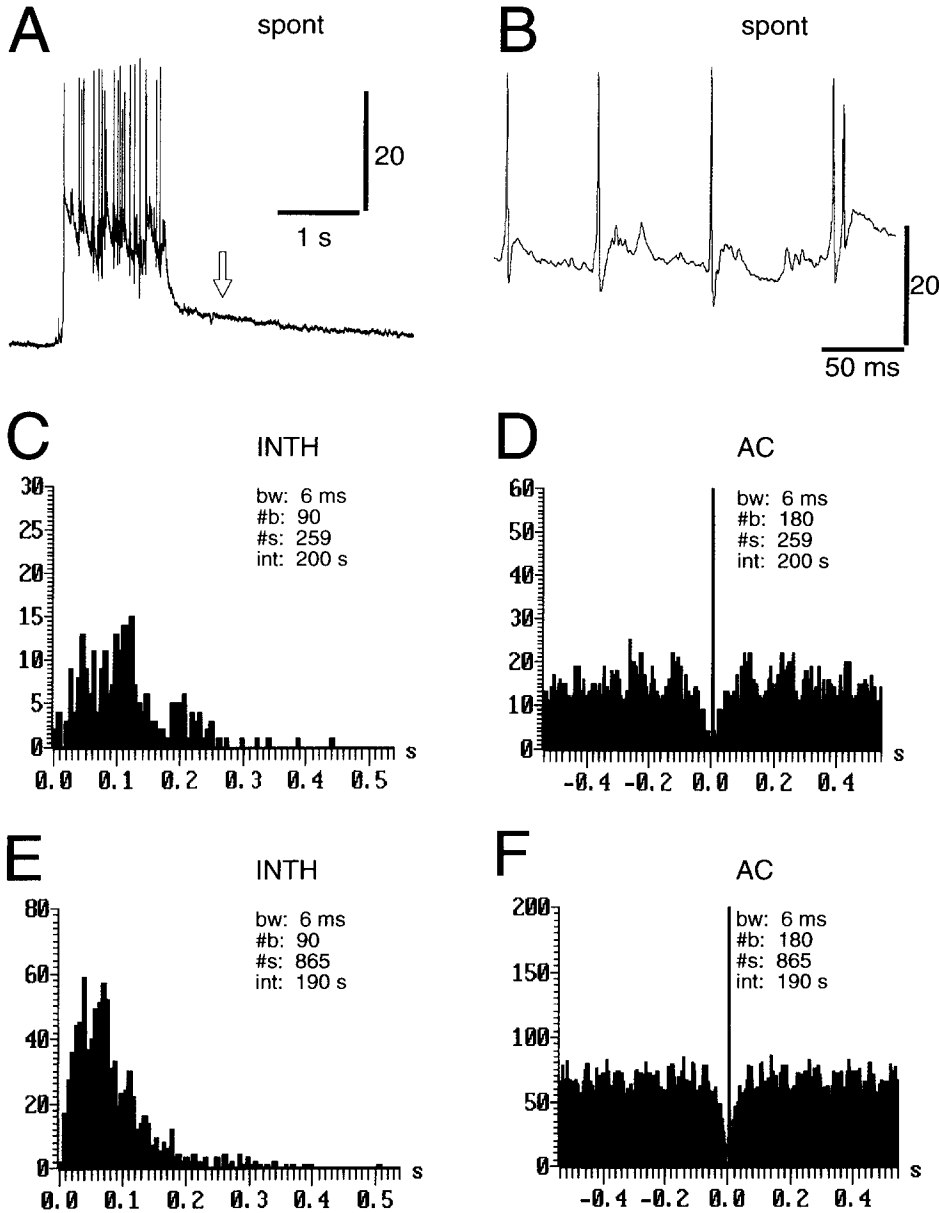


Fig. 6. Intracellular spontaneous activity in a cortical interneuron. (A) During depolarized periods strong spiking activity can be seen. (B) Magnified view of spiking activity during periods of high activity. (C) Spike interval histogram (INTH) of spontaneous activity. (D) AC reveals the presence of oscillatory activity. Spike interval histogram (E) and AC (F) during the first 190 s after weak, local blockade of non-*N*-methyl-D-aspartate receptors using 6-cyano-7-nitroquinoxaline-2,3-dione (CNQX; 1 s; 15 kPa). The oscillatory components are absent and the firing rate has more than tripled (cf. C, D).

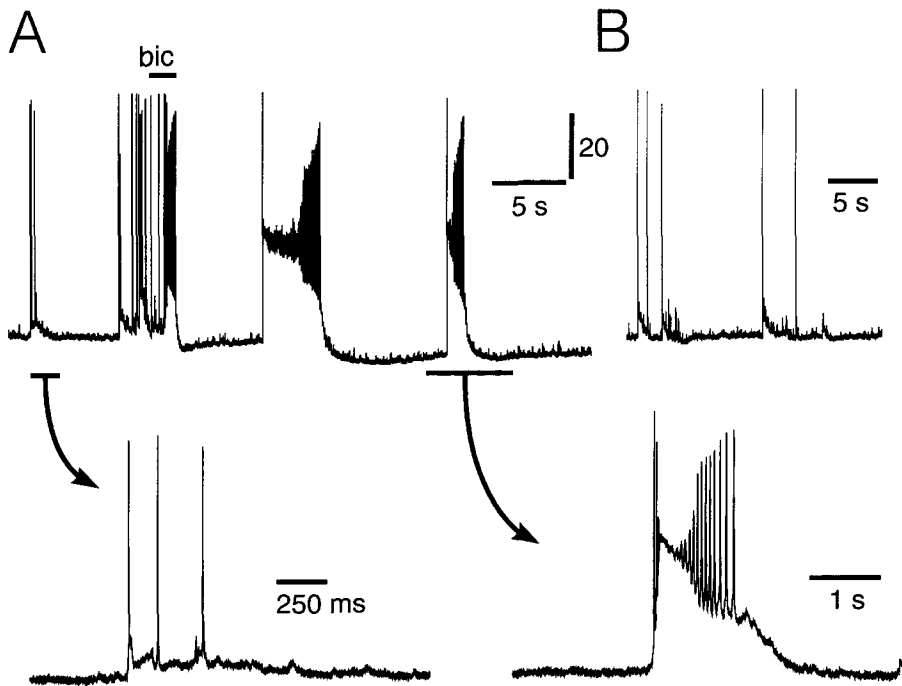


Fig. 7. Response of cortical neurons to removal of inhibition. (A) Spontaneous intracellular activity of a cortical cell shortly before and after local application of the GABA_A antagonist bicuculline (bic). Black bars below the time course indicate two regions of magnified view, shown in the lower traces. (B) Recovery after 1 min later.

It was also common to find principal cells in the depolarized state with moderate or no firing (Fig. 10C). Such cells might either have been in a condition of spike adaptation or, alternatively, the spontaneous net excitatory input might not have been sufficient to bring the cell to fire. Spike adaptation could be ruled out, as depolarization of those “silent” cells with a subthreshold current injection enabled the spontaneous inputs to cause the cells to fire strongly ($n = 9$; Fig. 10D). In order to test for GABA_A activity during the depolarized states, the GABA_A antagonist bicuculline was locally ejected one to several seconds after a cell became depolarized, abruptly increasing the firing in most cases (seven of 10), and thereby revealing peculiar dynamics: a local, temporary removal of GABA_Aergic inhibition enabled principal cells to sustain their high spike discharge to the end of a depolarization period. A new depolarization period “reset” these dynamics to the situation before bicuculline application (Fig. 10E). Furthermore, upon application of bicuculline the membrane potential depolarized and the membrane potential fluctuations during the depolarized state increased (Fig. 10E). In the other three cases, a short-lasting decrease in depolarizing potentials without any change in spiking was observed. In principal neurons postsynaptic potentials due to GABA_Aergic synaptic activity were positive with respect to the resting potential and reversed in polarity at -52 ± 1 mV ($n = 5$; Fig. 11A).

The depolarized state was also shown to exhibit

strong sensitivity to atropine. Local application of this muscarinic antagonist resulted in a destabilization of the “enabled” state in principal neurons (five of six; Fig. 11B). We attribute this destabilization of the depolarized state to local striatal effects; cortical and secondary striatal neurons ($n = 12$) did not show a decrease in activity after similar or even higher doses of atropine.

Striatal principal cells: extracellular recordings

Twenty-nine extracellular recordings were considered to be principal cells (Table 2), their firing behavior ranging from episodic bursting (Fig. 12A) to irregular spiking (Fig. 13A). In six cases unit activities from “silent” cells were recorded with a signal-to-noise ratio well beyond 3:1. These cells only spiked once within several minutes and could not be excited by cortical stimulation. No analysis of their spiking activity was done. The remaining 23 neurons showed a single-peaked spike interval histogram with an average modal interval of 124 ± 108 ms (Figs 12C, 13C, Table 2) and a complete inhibition in spiking activity for 85 ± 57 ms after a spike (Figs 12D, 13D). Twelve cells showed a characteristic decline in the AC (Fig. 12D, Table 2). The remaining cells showed only an irregular firing pattern in the AC, with no bursting activity visible (Fig. 13F). These latter cells were considered to be principal cells because of their single-peaked spike interval histograms and the absence of spike intervals shorter than 50 ms. Poststimulus time histograms were

calculated from 12 cells. Six cells showed an early single spike with a latency of 14 ± 7 ms. This early excitation was followed by a spike depression lasting for 80 ± 31 ms with a subsequent burst rebound, with peak excitation at 105 ± 54 ms (Fig. 12E, Table 2). In

a further two cells the same pattern was present except that the early spike was missing. These patterns are consistent with the intracellular recordings (cf. Fig. 9). A further four cells showed long-lasting depression upon cortical stimulation (Fig. 13E).

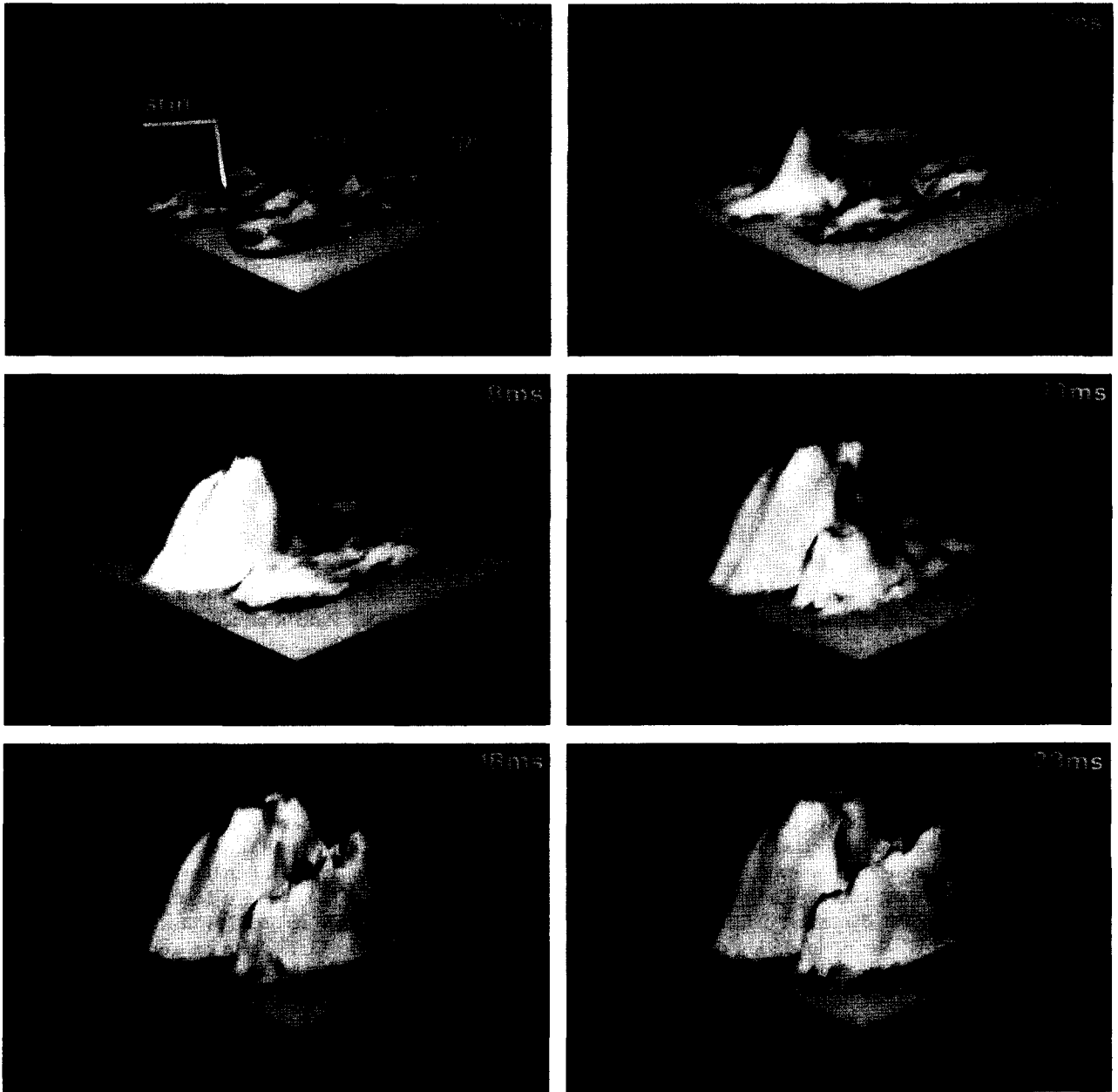


Fig. 8. Optical recording of the spreading of activity in a cortex-striatum co-culture (33 days *in vitro*, d33). The borders of the tissues are outlined in the activity plot taken 2 ms before stimulation (top left). Upward deflections in the profiles of relative fluorescence change (*z*-axis) indicate net depolarization. Each photodiode covers an area of $150 \times 150 \mu\text{m}$. Note the different spatial scales along the *x*- and *y*-axes. The sequence of activity profiles, taken at successive intervals of 5 ms and averaged over two stimuli presentations per location, shows the spread of activity in the co-culture upon electrical microstimulation in the cortex (stim). The small fluctuations in relative fluorescence change at 2 ms before stimulation give an indication of the noise level. At 3 ms after stimulation, a pronounced depolarization develops at the location of the stimulation electrode, and spreads over the cortical culture as time proceeds (cf. 8 ms and later). Again 5 ms later (13 ms), net depolarizing activity builds up in the striatal tissue adjoining the cortex, which spreads over the entire striatal culture in the following 10 ms (cf. 18 and 23 ms).

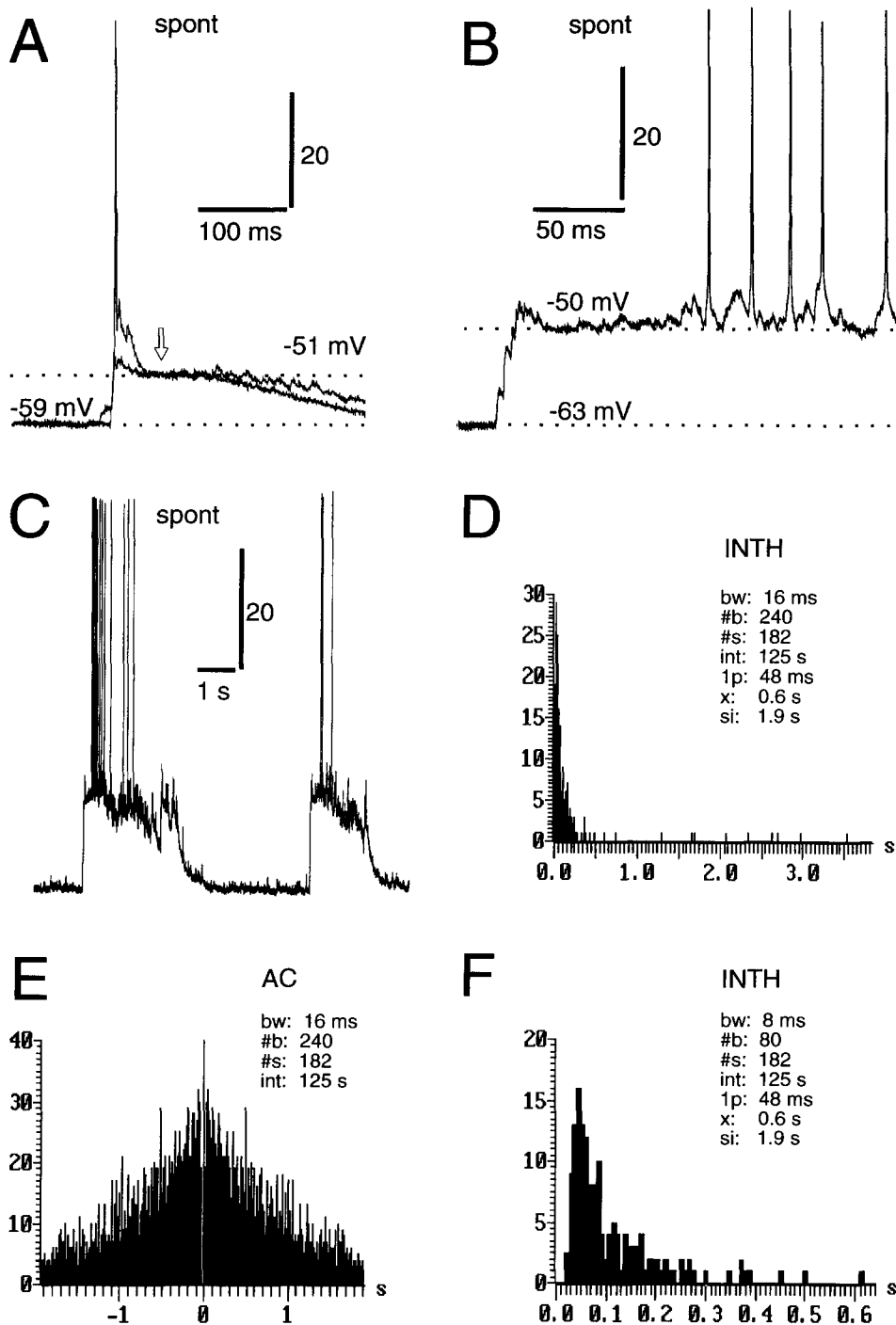


Fig. 9. Spontaneous intracellular membrane potential dynamics in striatal principal neurons. (A) Spontaneous sub- and suprathreshold events in a principal neuron superimposed. After an early sub- or suprathreshold excitation, a short-lasting subthreshold stabilization of the membrane potential (arrow) is clearly visible. (B) Principal cell showing periods of spiking activity (C) after becoming depolarized. Spiking activity develops after an early period of spike depression. Spike interval histograms (D, F) and AC (E) of the principal neuron shown in B and C reveal typical characteristics of firing behavior in bursts. No interspike intervals below 20 ms are present.

Striatal secondary type I neurons

Secondary type I cells are most likely to represent the class of the striatal GABAergic interneuron (see Ref. 104a). In these neurons the average maximum

spike discharge was two- to three-times higher than in principal neurons (eight to 12 spikes per second). The spike interval histogram revealed an average intraburst interspike interval of around 9 ms

(Table 3) In type I neurons two stereotyped spiking patterns were present.

The first pattern was characterized by short-lasting, high-frequency bursts (Fig. 14) upon slight depolarizations and prominent AHPs (Fig. 14A, B). The spike interval histogram showed an early peak with a steep decline towards larger interval values (Fig. 14C, E). Occasionally, a second, broader peak was present at 100–200 ms. The AC, besides reproducing the characteristic time course of the spike interval histogram, additionally indicated irregular interburst intervals (Fig. 14D). The burst duration ranged from 30 to 50 ms (Table 3) and was much shorter than in principal cells. This highly stereotyped bursting behavior was also present in extracellular recordings. Spontaneous, short-lasting bursts with small intraburst intervals led to spike interval histograms and ACs almost identical to those described for the intracellular recordings (Fig. 15A–D). Cortical microstimulation elicited an early burst, followed by a spike depression and subsequent long-lasting excitation (Fig. 15E, F, Table 3); this pattern was also present in the intracellular recordings of spontaneous activity (cf. Fig. 14A).

The second pattern also reflected strongly bursting neurons with small intraburst spike intervals. In addition the spontaneous membrane potential time course revealed outward rectification and spike depression, which was especially obvious after single spikes (Fig. 16A, B). The spike interval histogram was double-peaked with an early peak at 8 ms, indicating the intraburst interval and a second modal

interval at 100 ms (Fig. 16C, E; cf. Table 3). Apart from the initial early peak at 8 ms, an overall decrease in spike discharge lasting several tens of milliseconds was visible in the AC (Fig. 16D, Table 3) with 7–15 Hz oscillatory components present (Table 3, Fig. 16D: about 15 Hz). The characteristic spike depression and membrane rectification was also revealed in neurons showing no oscillatory activity at all (Fig. 16E, F). This second pattern was again found in the extracellular recordings (Fig. 17). The spontaneous activity was characterized by 1–2 s bursting activity and a biphasic unit wave form (Fig. 17A, B). Spike interval histograms and ACs revealed the tendency to fire in high-frequency bursts with early spike depression and oscillatory activity at approximately 12 Hz (Table 3, Fig. 17C, D: 15 Hz).

Type I cells received strong inhibitory inputs, which was particularly evident in relatively polarized cells. Barrages of inhibitory synaptic input were seen to briefly disrupt spike discharges (Fig. 17E, F). Both type Ia (all of six) and type Ib (all of four) neurons responded to short bicuculline applications with an immediate increase of spike discharge (10 ± 5 and 6 ± 3 spikes/s, respectively; Fig. 17G).

Striatal secondary type II neurons

These cells represent striatal cholinergic interneurons (see Ref. 104a). Of 15 neurons characterized, eight were used for statistical analysis of their spontaneous discharge. The maximum average discharge was four to five spikes per second (Table 4). Spontaneous discharge was irregular and

Table 2. Spiking activity of striatal principal neurons in cortex–striatum co-cultures

	Intracellular	<i>n</i>	Extracellular	<i>n</i>
Age (days)	25 ± 5	11	27 ± 3	29
Fmax† (spikes/s)*	3.0 ± 1.4	11	4.6 ± 3.3	23
INTH‡ (ms)*	96 ± 72	11	124 ± 108	23
Mean (s)§	3.4 ± 0.9	11	1.1 ± 0.6	23
Sig (s)§	6.2 ± 5.5	11	3.1 ± 1.6	23
AC int (ms)*	1080 ± 460	11	840 ± 460	12
PSTH exc¶ (ms)	—	—	14 ± 7	6
PSTH inh** (ms)	—	—	81 ± 28	8
PSTH reb†† (ms)	—	—	115 ± 57	8
PSTH inh‡‡ (ms)	—	—	1540 ± 1900	4

*Not different at $P < 0.05$; two-tailed Wilcoxon's rank sum test.

†Maximum firing rate, calculated by using a sliding integration window (integration width: 3 s) and taking peak value.

‡Modal interval in the spike interval histogram.

§The mean and S.D. of the spike interval histogram. Under the assumption of a Poisson process both values should be equal.

||Average burst length as determined from the AC. A linear fit was made to the decline in the AC during the first 500 ms after maximum spiking probability was calculated. The intersection of this linear fit with the time axis, calculated by interpolation, was taken as an approximation of the burst length.

¶Time from cortical stimulation to the early, single peak in the poststimulus time histogram (PSTH).

**Time from early single peak in the poststimulus time histogram to end of complete discharge inhibition.

††Time from cortical stimulation to maximum discharge peak in poststimulus time histogram, following the period of discharge inhibition.

‡‡Time from cortical stimulation to the end of discharge inhibition.

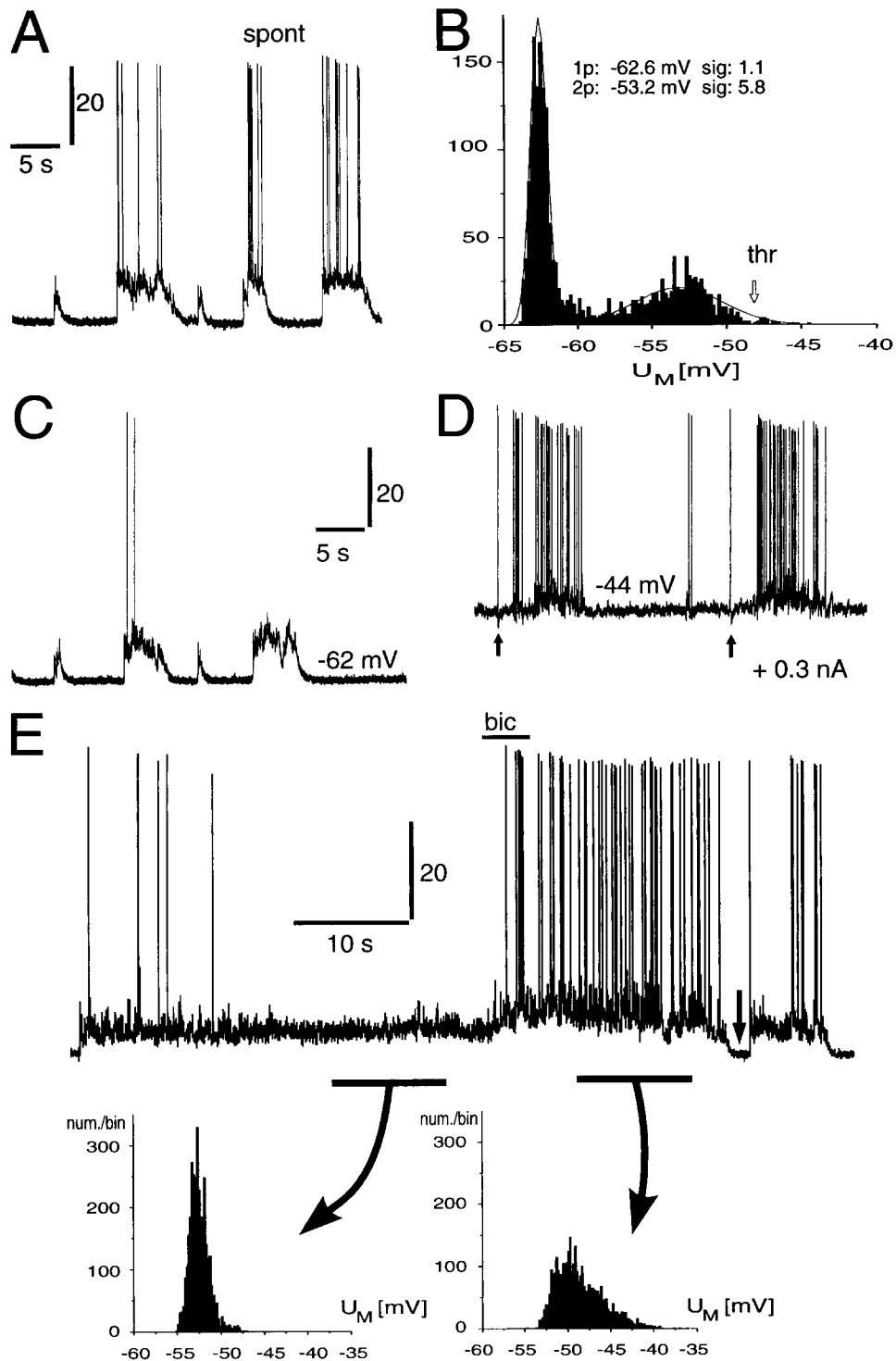


Fig. 10. Spontaneous intracellular membrane potential dynamics in principal neurons and its sensitivity to $GABA_A$ blockade. (A) Spontaneous activity in a principal neuron. Episodic burst activity occurs during the depolarized state. (B) Membrane potential distribution of trace shown in A clearly reveals a bi-modal distribution, with one peak at the resting potential and a second one which steeply declines towards threshold (thr). The membrane potential value was sampled at 2 ms intervals. For comparison, Gaussian curves were fitted to each peak, indicating the means (1p and 2p) and the standard deviations (sig). (C) Principal neuron showing only moderate spiking activity during depolarized states. (D) During a constant, subthreshold current injection (+0.3 nA), which depolarizes the neuron to -44 mV, periods of strong firing due to background activity are present. Same neuron and scale as in C. Note that under these relatively depolarized conditions a short-lasting hyperpolarization after single spikes, with subsequent spike depression, followed by a long-lasting rebound excitation are revealed (arrows). (E) Principal neuron showing only a few spikes at the beginning of the depolarized state. Upon local injection of bicuculline (bic) this neuron enters a sustained period of strong firing. With the beginning of a new period of depolarization (arrow), the firing behavior is reset to the level observed before the bicuculline application. Horizontal bars below the trace indicate intervals used for membrane potential distributions before (bottom left) and after (bottom right) bicuculline application (sampled at 0.2 ms intervals). Upon local blockade of $GABA_A$ receptors, the neuron depolarizes and the range of membrane potential fluctuations broadens.

tonic during periods of depolarization, with occasional spike doublets (Fig. 18A, B). Outward rectification was not present; however, after a spike the membrane potential underwent long-lasting hyperpolarizations (Fig. 18B, arrows) restricting the maximal spike discharge. All neurons showed a narrow, early peak in the spike interval histogram and in the AC (Fig. 18C–F, Table 4). This discharge behavior was much more variable than in secondary type I neurons, with the main difference arising from the amount of early spike depression seen in the ACs. The ACs of secondary type II neurons most closely resembled those of pyramidal neurons, except for the occurrences of double spikes. In contrast to secondary type I neurons, secondary type II neurons did not seem to receive any strong GABA_Aergic inhibition, as no change in firing was detected upon local application of bicuculline (all of five neurons).

Crosscorrelations in the striatal part of cortex–striatum co-cultures

Multi-unit activities recorded using one or two electrodes were crosscorrelated ($n = 11$), revealing a strong and selective synchronization among striatal type I and principal cells (all of four), even between distant units (Fig. 19). The spike interval histogram of the first unit classified this unit as a type I neuron. The second unit showed a similar burst-like firing to unit 1 (Fig. 19A, upper trace); however, the spike interval histogram of unit 2 was typical for principal cells: it was single-peaked and no spike intervals smaller than 50 ms occurred (Fig. 19D; compare Figs 9, 12C, 13C). The spontaneous activity of the third unit showed a quite different activity than those of units 1 and 2 (Fig. 19A, upper trace) and the spike interval histogram of unit 3 was also typical for principal cells (Fig. 19F). Both ACs of units 2 and 3 showed a decline during the first second that is typical

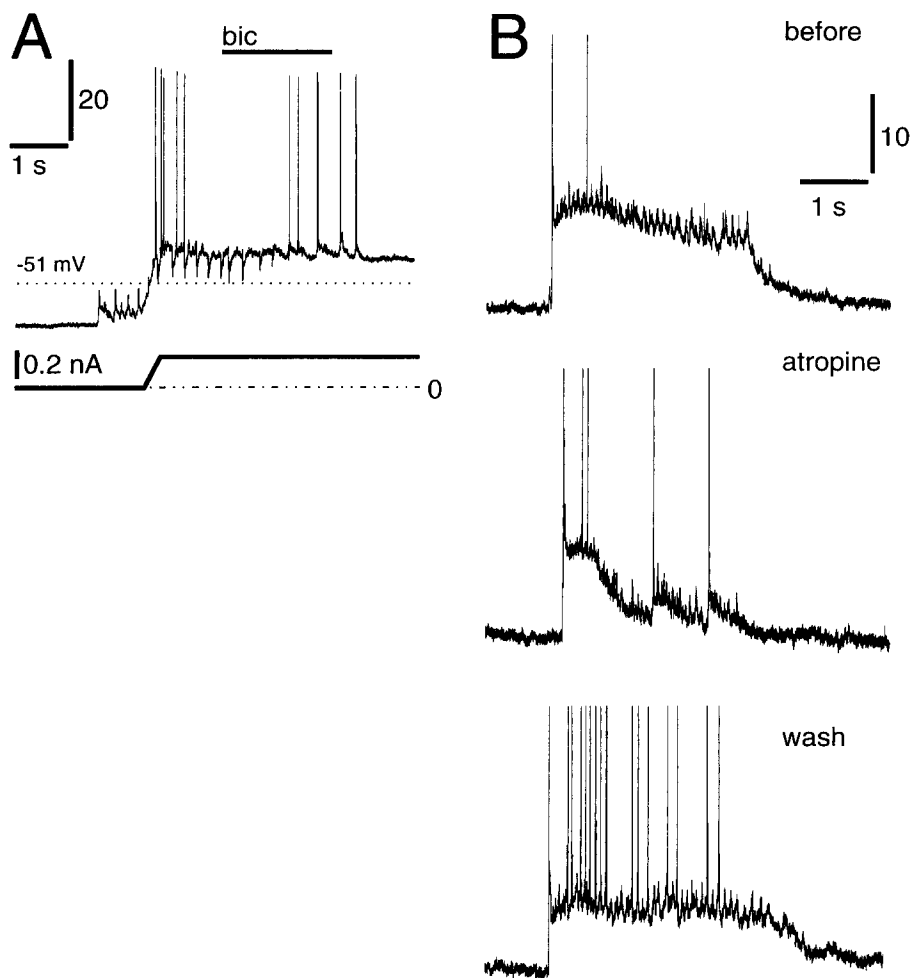


Fig. 11. Reversal of spontaneous GABA_A synaptic potentials and sensitivity of the depolarized state to local blockade of muscarinic activity in principal neurons. (A) Spontaneous depolarizing events in a principal neuron reverse upon artificial depolarization above -51 mV. Reversal potentials are sensitive to locally ejected bicuculline (bic). Upper trace: membrane potential. Lower trace: current injection. (B) “Enabled” state in a principal neuron shown shortly before (top), 6 s after (middle) and 1 min after (bottom) local injection of the muscarinic antagonist atropine (2 s; 20 kPa; spikes are truncated).

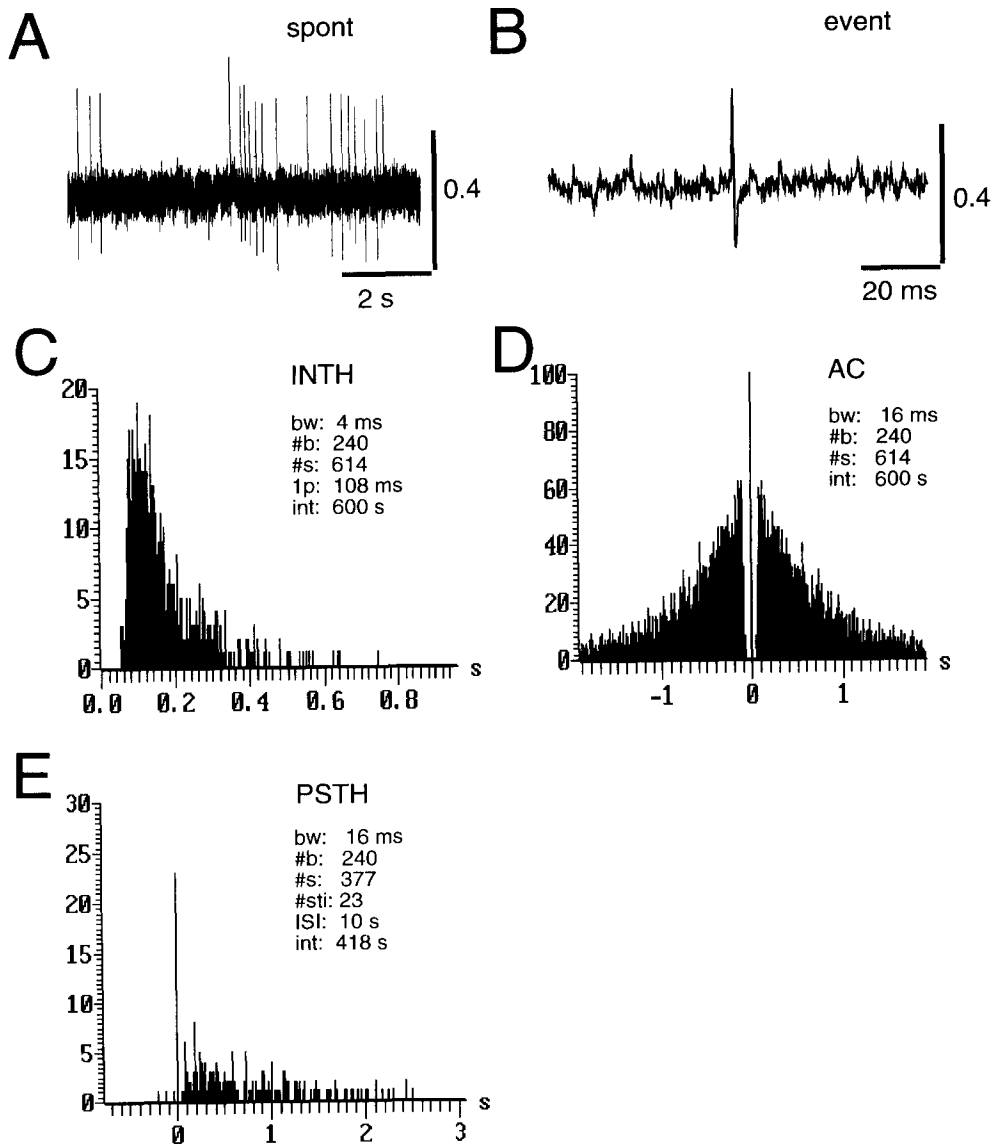


Fig. 12. Extracellular single-unit activity in striatal principal neurons (bursting). (A) Spontaneous spiking. (B) Biphasic time course of single unit with positive (upward) deflection first. (C) Spike interval histogram of the unit shown in A. The single-peaked distribution reveals a clear predominance of interspike intervals around 100 ms and an absence of intervals shorter than 48 ms. (D) The AC reveals a strong decline in discharge probability during the first second after a spike. (E) Poststimulus time histogram reveals an early single peak, followed by a short-lasting spike inhibition with subsequent rebound excitation upon cortical stimulation.

for principal neurons (data not shown). The CC revealed a highly selective synchronization among these three units. Units 1 and 2 had tightly synchronized spikes, as indicated by the prominent narrow central peak in the CC (Fig. 19C, E). In contrast, the CC of units 3 and 1 showed only weak synchronization (Fig. 19G), yet prolonged discharge periods in unit 3 either stopped or started after short-lasting synchronized group discharges of units 1 and 2 (Fig. 19A, dot display above the spike traces).

DISCUSSION

Organotypic cortex–striatum co-cultures provide an *in vitro* model to study corticostriatal dynamics. In this model the cortical network is the main source of activity. We will therefore first discuss the features of the cortical dynamics, before describing the dynamics of the striatal network and the way these are influenced by cortical activity.

Spontaneous activity in isolated single cortices

Chronically isolated slabs of cortical regions in adult brains differ in electroencephalographic activity recorded from cortical regions outside the isolated area.⁴⁰ They express patterns of highly activity periods ("bursts"), separated by silent periods, or repetitive discharges reminiscent of activity recorded from epileptogenic foci. Immature neocortical regions express similar unique and stable patterns of

field potential activity within days after isolation.¹⁰⁸ Such patterns were considered to result from an overconnectivity within the isolated region²² and to indicate the presence of "... relatively stable synaptic pathways ... [constituting] ... preferential circuits of transmission of activity"¹⁰⁸ in the cortical network.

These early indications of stable, repetitive states of activity in isolated cortical networks have been confirmed in a number of investigations using organo-

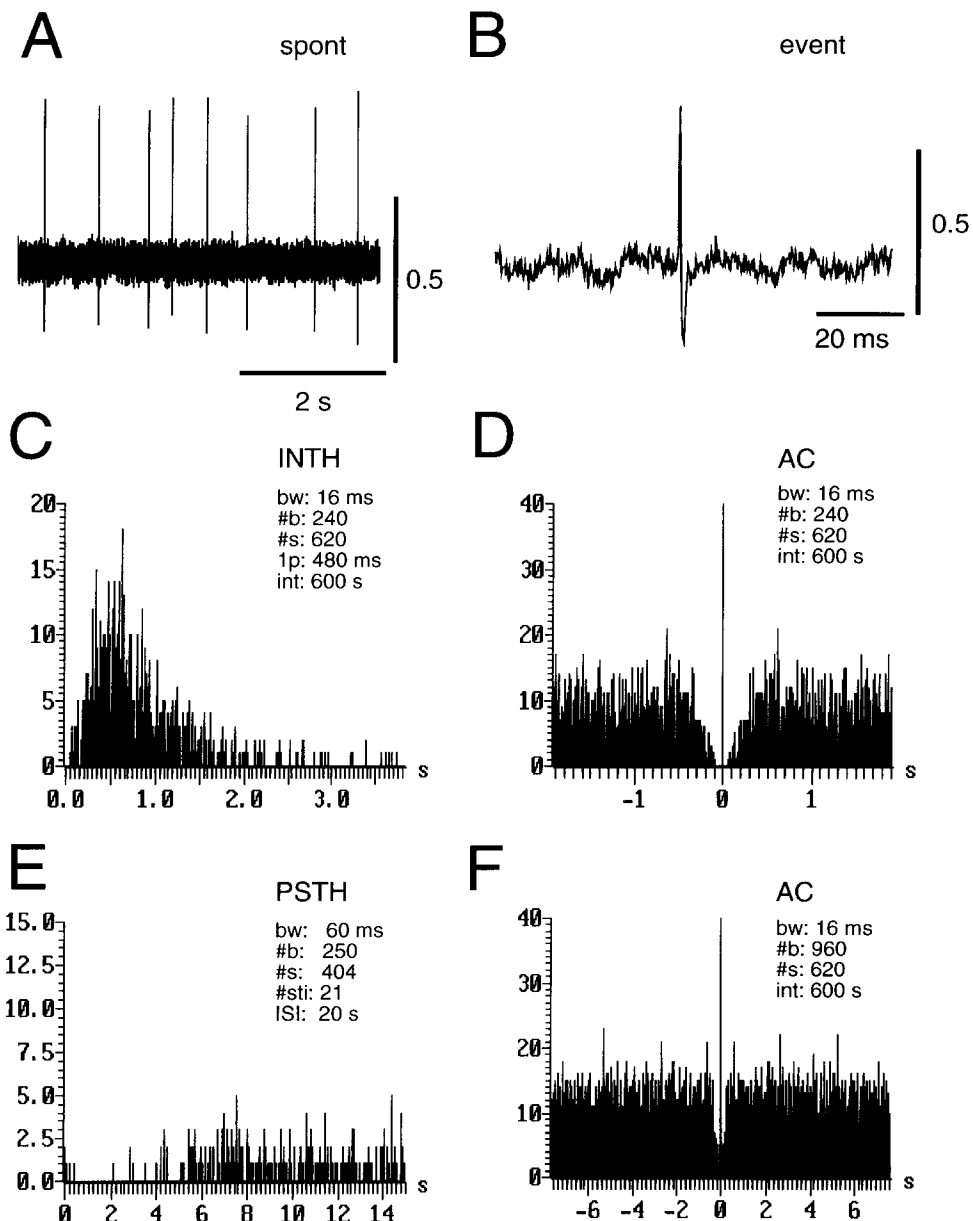


Fig. 13. Extracellular single-unit activity in striatal principal neurons (irregular firing). (A) Spontaneous, irregular spiking activity at low rates. (B) Biphasic time course of single unit with positive (upward) deflection first. (C) Spike interval histogram of the unit shown in A. The single-peaked distribution reveals a clear predominance of spike intervals around 500 ms and an absence of intervals shorter than 48 ms. (D) The AC reveals a strong decrease in discharge probability during the first 400 ms after a spike. (E) Poststimulus time histogram reveals a long-lasting inhibition of spike discharge upon cortical stimulation. (F) The flat time course in the AC shows the spontaneous, irregular, non-bursting firing mode of this neuron.

Table 3. Spiking activity of striatal secondary type Ia and Ib neurons in cortex–striatum co-cultures

	Intracellular				Extracellular	n
	Secondary type Ia	n	Secondary type Ib	n		
Age (days)	23 ± 3	9	22 ± 3	8	30 ± 5	8
Fmax† (spikes/s)*	8 ± 3	9	12 ± 8	8	13 ± 5	8
INTH‡ 1p (ms)*	8.9 ± 2.5	9	8.2 ± 1.2	8	8.1 ± 5.7	5
INTH‡ 2p (ms)*	121 ± 40	4	86 ± 50	8	138 ± 83	6
AC int§ (ms)*	50 ± 19	6	32 ± 9	4	33 ± 10	4
Δt (ms)*	71 ± 38	3	53 ± 18	4	874 ± 54	4
osc¶ (Hz)	8.4 ± 1.9	3	13.4 ± 2.1	4	11.5 ± 4.1	4
PSTH exc** (ms)	—	—	—	—	11 ± 3	5
PSTH inh†† (ms)	—	—	—	—	167 ± 85	5
PSTH reb‡‡ (ms)	—	—	—	—	188 ± 92	5

*Not different at $P < 0.05$; two-tailed Wilcoxon's rank sum test.

†Maximum firing rate, calculated by using a sliding integration window (integration width: 3 s) and taking peak value.

‡Interval at first (1p) or second peak (2p) in the spike interval histogram (INTH).

§Average burst length as determined from the AC. A linear fit to the decline in the AC during the first 500 ms after maximum spiking probability was calculated. The intersection of this linear fit with the time axis, calculated by interpolation, was taken as an approximation of the burst length.

||Duration of depression in spike discharge, which persists for several tens of milliseconds after the first peak in the AC. Time was taken from the intersection with the baseline in the AC.

¶Oscillatory frequency derived from the interval between successive peaks in the AC.

**Time from cortical stimulation to the early peak in poststimulus time histogram (PSTH).

††Time from early peak in poststimulus time histogram to the end of discharge inhibition.

typic single neocortical cultures.^{26,36,79} The activity patterns seen are considered to reflect the underlying synchronization of synaptic activity in groups of pyramidal neurons.^{26,35,52} These particular dynamics in field potentials and spike discharges have also been reported *in vivo*⁴¹ and in cortical neural network simulations incorporating excitatory and inhibitory neurons.⁴² The present study demonstrates that such changes in spontaneous discharge, with underlying polysynaptic activity, near-coincident firing and stable states of activity transmission induced by cortical microstimulation, are also characteristic features of the cortical dynamics in the cortex–striatum co-cultures.

Comparison with cortical dynamics *in vivo*

The dynamics described here for the cortical part of the co-culture have remarkable similarities to certain cortical dynamics *in vivo*. In urethane-anesthetized animals^{43,92} and during slow-wave sleep,^{37,43} cortical activity in deeper layers is characterized by a burst–pause pattern (for a review see Steriade *et al.*¹²¹). Burst duration ranges up to 2 s with two to nine spikes per burst,¹⁰ giving spike rates of two to eight spikes per second.⁵⁷ During bursts, cortical neurons which are uncorrelated or weakly correlated during wakefulness show strong common correlation in spiking activity.^{57,96} Burst–pause patterns with average spiking activity of three to four spikes per second during bursts and strong correlations in spike discharge are also characteristic features of the spontaneous activity in the cortical culture described in this study.

Epileptic discharge

Suboptimal conditions during culturing can easily induce epileptic discharge in neocortical explants.^{106,107} In particular, immature neocortical neurons are likely to express epileptic activity,^{54,74} but even when fully matured, anoxic conditions can still selectively destroy GABAergic interneurons, leading to hyperexcitability.¹¹⁴ In our studies, cortical tissue parts with dimensions two- to three-times as broad as they were deep proved to be optimal for culturing, and only occasionally were seizure-like episodes⁵² observed. Thus, most of the activity examined in the co-culture system was different from epileptic discharge. This is in agreement with the general finding that, despite the susceptibility of neocortical explants, stable epileptic activity involving calcium entry¹⁴ and *N*-methyl-D-aspartate receptor activation^{11,52} has to be induced by convulsants (see also this study).

The role of GABAergic interneurons in cortical dynamics

In dissociated cultures it was shown that discontinuous firing modes, up to the extreme case of burst–pause patterns, establish after three weeks in culture, i.e. at a time when GABAergic neurons have matured.⁵³ Similar parallels to the maturation of GABAergic neurons⁴⁸ and the complexity in spontaneous bioelectric activity^{35,36} exist for organotypic single-cortex cultures. Immunohistochemical results²⁷ (see Ref. 104a), the electrophysiological evidence presented in this study and the effect of bicuculline as a strong convulsant^{11,144} demonstrate

the presence of a strong inhibition in organotypic cortex cultures after at least three weeks *in vitro*. This suggests that the maturation of a recurrent local feedback loop among pyramidal neurons and interneurons is a prerequisite for the spontaneous grouping in spiking activity among pyramidal neurons. Synchronized inhibition, lasting in the range of 100 ms, has been proposed as a mechanism for

grouping neuronal discharge into repetitive slow, oscillatory activity:⁶ recent computer simulations have been synchronized inhibition to be highly effective in producing such group discharge.⁸⁴ In our preparation the recurrent local feedback loop between pyramidal cells and inhibitory interneurons might also be responsible for the predominant interspike interval in the range of 80–120 ms observed in

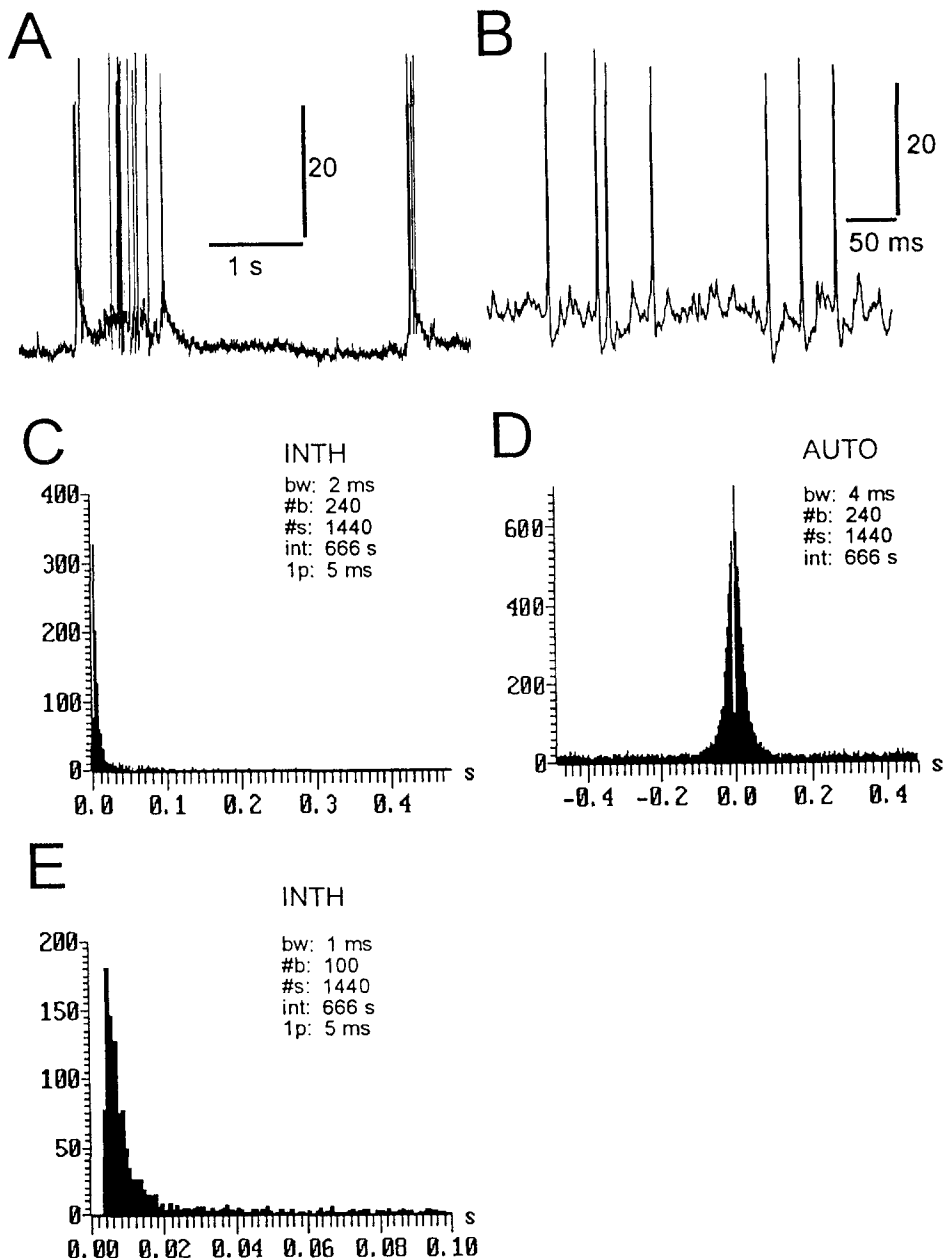


Fig. 14. Spontaneous intracellular membrane potential dynamics in striatal type I neurons (early spike depression absent). (A) One complete high activity period and the beginning of a second one are shown. Bursting occurs immediately upon depolarization onset, and is followed by a period of spike depression with subsequent long-lasting rebound excitation. (B) Magnified view of spiking during high activity period. Prominent AHPs are present, but no membrane rectification is visible. The narrow, single-peaked distribution in the spike interval histogram (C, E) reveals a clear predominance of a regular, very short spike interval around 5 ms. (D) The AC shows a strong decline in spiking probability within the first 40 ms after a spike, pointing at a short burst duration. At longer times the AC is flat.

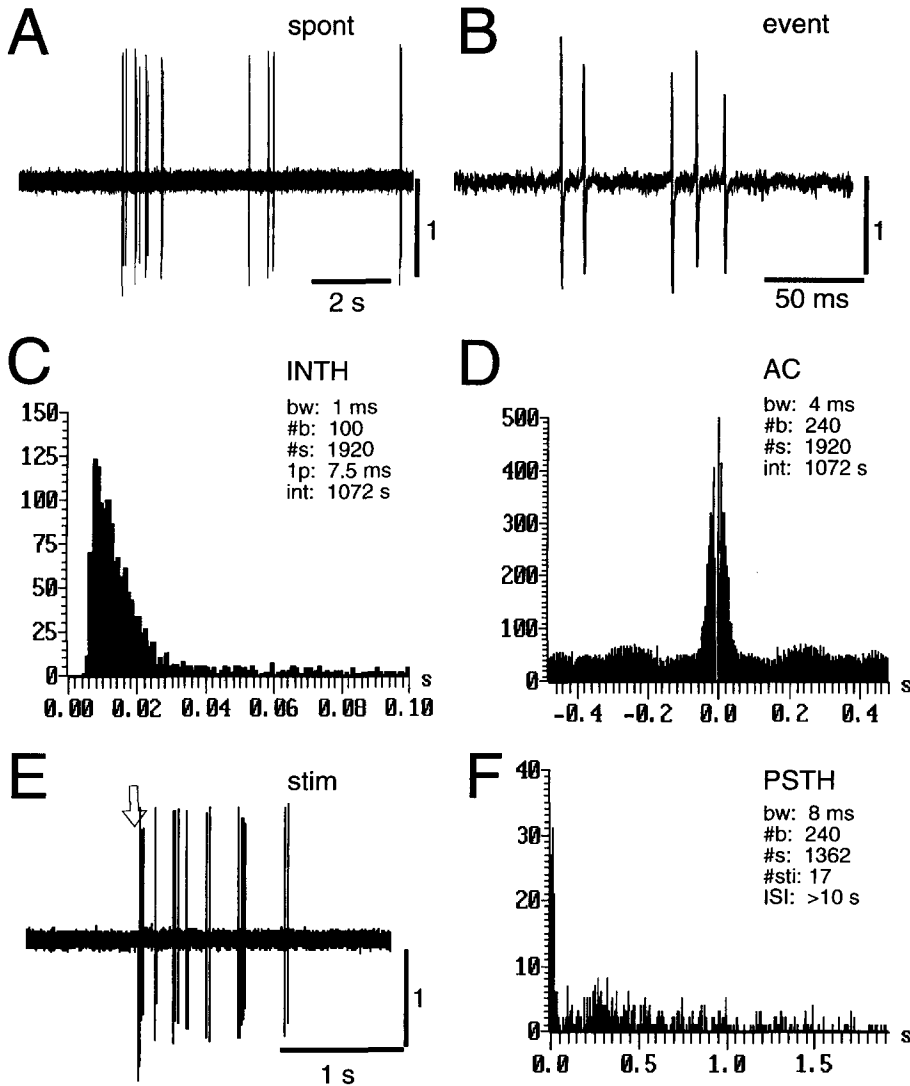


Fig. 15. Extracellular single-unit activity in striatal secondary type I neurons (early spike depression absent). (A) Spontaneous bursting. (B) Biphasic time course of single units with positive (upward) deflection first. Note the regular intra-burst spike interval. (C) Spike interval histogram of the unit shown in A. The single-peaked distribution reveals a regular intra-burst spike interval of 8 ms. The distribution steeply declines to base level at intervals larger than 30 ms. (D) The AC reveals a strong decline in discharge probability during the first 50 ms after a spike, indicating a short burst duration. (E) Cortical stimulation induces a period of bursting activity, similar to the spontaneous activity shown in A and Fig. 14A. (F) The poststimulus time histogram upon stimulation reveals an early burst of spikes, followed by a spike depression with subsequent rebound excitation.

pyramidal neurons. This view is supported by the oscillatory discharge at 8–9 Hz present in the cortical interneuron.

Spontaneous activity in principal neurons

Despite some similarities between principal cells and pyramidal cells (e.g. spike width, spike AHP, average firing rate), the spiking behavior of principal cells was unique and not predictable from cortical firing (cf. e.g. secondary type II neurons). The ACs and spike interval histograms described in this study are very similar to spike interval histograms and ACs derived from intracellularly identified and uniden-

tified striatal principal cells in urethane-anesthetized rats.^{137,142} Burst durations up to 3 s, absence of interspike intervals smaller than 8–20 ms and modal interspike intervals ranging from 8 to 75 ms are typical features *in vivo*, and were also expressed in the co-culture system. Similar ACs have been reported in immobilized, awake rats for striatal units showing “group” discharge⁴⁷ and, in awake monkeys, episodic bursting² and single-peaked spike interval histograms in the range below 100 ms^{65,67} have been described for striatal projection neurons.

In the co-cultures, dopaminergic input is absent. Since dopamine deficiency is known to increase the

number of principal neurons firing at higher rates,⁹⁴ one might expect principal neurons in the striatal tissue part to fire at abnormally high rates. However, the average firing rates we found are well within the range reported for anesthetized rats.¹⁴²

Our findings from intracellular recordings were reproduced in the extracellular recordings. In the latter case we also found cells with very low spiking activity which could not be excited by cortical stimu-

lation. These units might be principal cells, as similar dynamics were found in the intracellular recordings (Fig. 10C). Single units with very low firing rates, a characteristics of striatal activity *in vivo* and also expressed in the co-culture system, have been reported since early studies on striatal spontaneous activity.^{e.g. 16} Such units with low firing rates are generally assumed to be principal projection neurons.

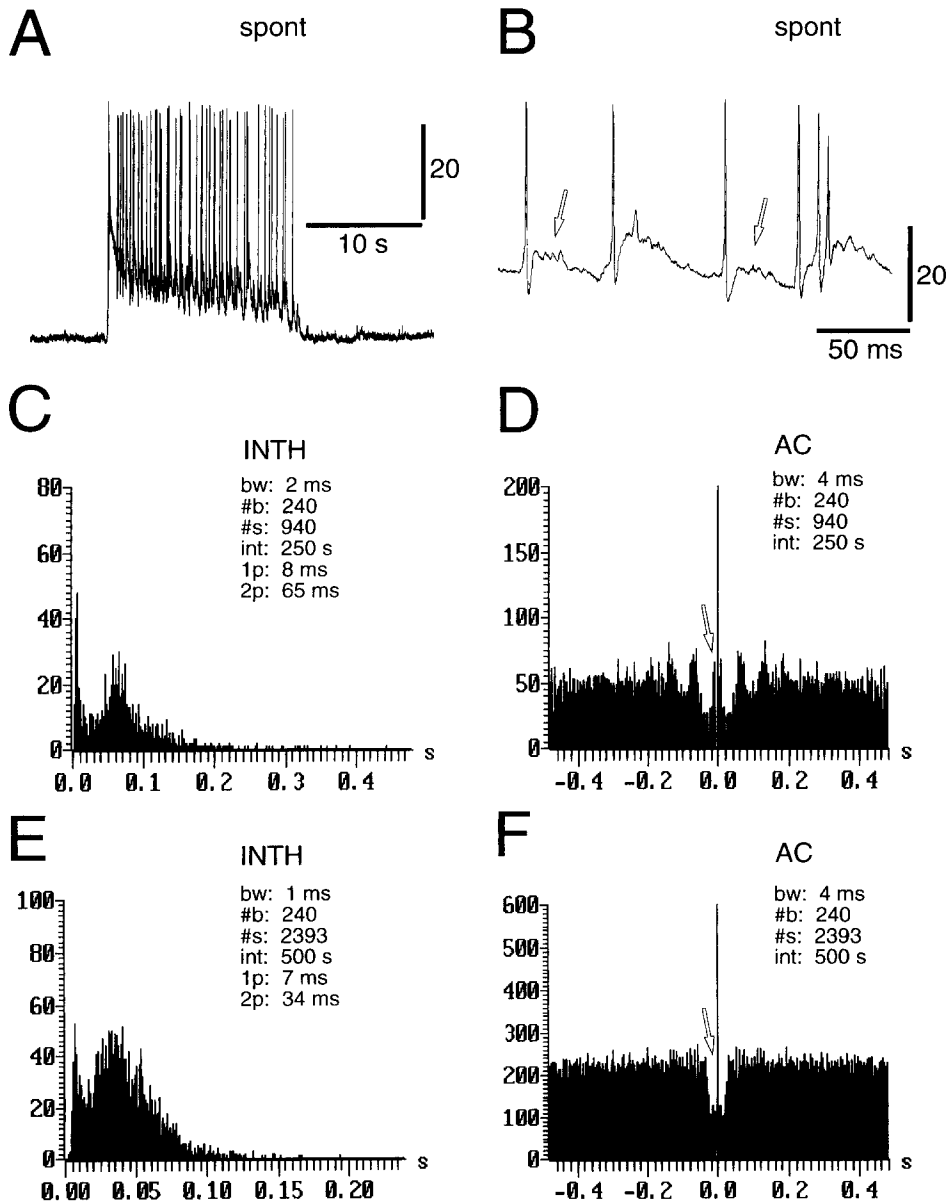


Fig. 16. Spontaneous intracellular membrane potential dynamics in striatal secondary type I neurons (early spike depression present). (A) Period of high activity in a type Ib neuron. The spiking activity is composed of isolated spikes and bursts. In particular, isolated spikes are followed by a characteristic membrane potential rectification (B, arrows). (C) The double-peaked distribution in the spike interval histogram reveals a prominent intra-burst spike interval of 8 ms and a second modal interval at 65 ms. (D) The AC, besides having an early peak at 8 ms (arrow), shows a strong depression in spiking probability during the first 120 ms and oscillatory activity in the range of 15 Hz. Double-peaked spike interval histogram (E) and AC (F) of another type I neuron illustrate a case without any oscillatory activity present.

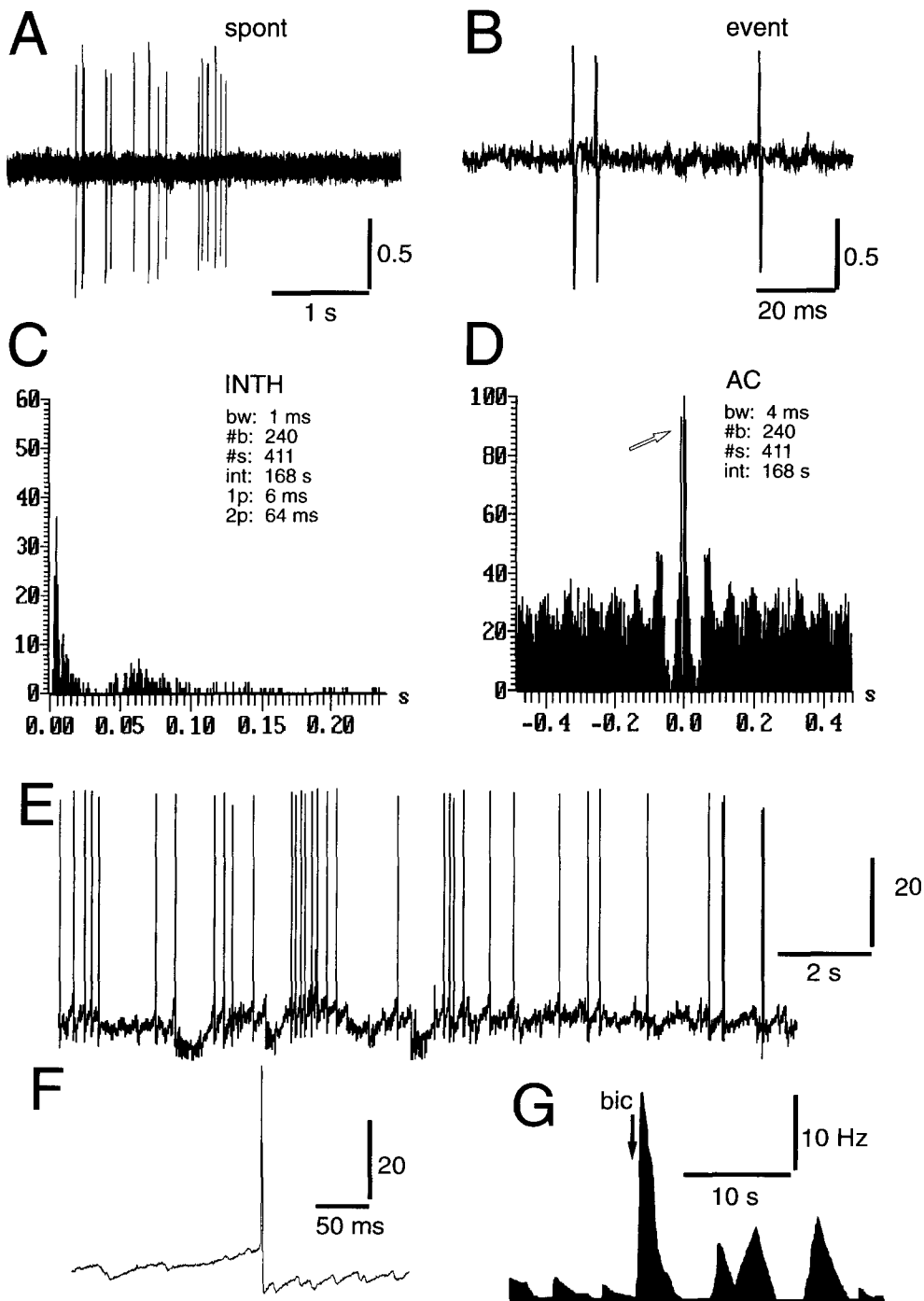


Fig. 17. Extracellular single-unit activity in striatal secondary type I neurons (early spike depression present) and its sensitivity to local GABA_A blockade. (A) Spontaneous bursting. (B) Biphasic time course of single units with positive (upward) deflection first. (C) The double-peaked spike interval histogram reveals a short intra-burst spike interval at 6 ms and a second modal interval at 64 ms. (D) The AC, besides having an early peak at 6 ms (arrow), shows a strong depression in spiking probability during the first 60–100 ms and exhibits oscillatory 15 Hz activity. (E–G) Spontaneous intracellular recording of a secondary type Ia neuron, revealing barrages of hyperpolarizing synaptic input. Local application of bicuculline (bic; 1 s, 25 kPa) leads to an abrupt increase in spike discharge followed by long-lasting changes in spontaneous activity (integration width: 1 s).

Enabled state and the occurrences of bursts in principal neurons

Particular membrane potential dynamics in striatal principal cells were first described by Wilson for the urethane-anesthetized rat *in vivo*:^{136,137,142} spiking activity only developed during the depolarized state, which was therefore called the “enabled” state; the very polarized state, with no spiking activity present, was called the “disabled” state.¹³⁷ Similar dynamics were also demonstrated for principal cells in the co-culture system. When considering these intracellular dynamics, one has to differentiate between mechanisms which bring the principal cells into the enabled state, and those that keep the membrane potential within that narrow polarized range.

Computer simulations have led to the proposal that a positive-feedback loop between a decrement of the “anomalous rectifier” conductance and synaptic, synchronized input leads to a fast transition from the polarized to the depolarized state.¹³⁶ Such fast transitions were readily observed in the principal cells of the co-culture (cf. Figs 9, 10). After such a transition, principal cells remained in the subthreshold range, eliciting at most a single spike during the very early depolarization (Fig. 8B, C).

Whether a principal neuron bursts or not, once in the “enabled” state, depends on the spatiotemporal patterns of excitatory and inhibitory inputs,¹²² balanced by intrinsic membrane currents.^{12,25,123-125} In this study, we have focused on synaptic inhibition during late phases in the “enabled” state. The rationale for this particular protocol was the following: if intrinsic, slowly changing currents govern the burst occurrences in principal cells, such intrinsic control would dominate during the first half a second after entering the depolarized state. After that, principal neurons and GABAergic interneurons will burst and

the resulting inhibition should prevent other principal neurons from spiking. In this case, given the presence of appropriate excitatory input, local removal of GABAergic inhibition should result in firing. This was observed in the striatal part of the culture (Fig. 10E). Thus, we conclude that the low spiking activity in the enabled state is not exclusively due to intrinsic membrane currents, but rather reflects a balance in excitatory and inhibitory inputs. Furthermore, the abrupt increase in membrane depolarization and firing rate outlasted the bicuculline pulse and was “reset” with a new period of depolarization. Such short-term “memory” might result if the neuron which was enabled to fire now inhibits other neurons, thereby disinhibiting itself. Such dynamics were, in fact, proposed on the basis of several theoretical studies on lateral inhibitory networks.^{4,91,133,134}

Reversal potential of GABA_A synapses and shunting inhibition in principal cells

The narrow membrane potential distribution in the “enabled” state, which broadens upon local application of bicuculline, is a strong indication of the GABAergic shunting activity. We show here that the reversal potential of GABA_A-sensitive potentials in principal cells lies within the subthreshold, depolarized range of the “enabled” state. Obviously, this value can only be an approximation, since temperature shifts changing active transport efficacy,¹²⁶ maturation,^{31,83} activity levels,^{127,128} masking by co-activated excitatory synapses⁹⁰ and locally restricted chloride-gradient shifts¹⁰⁹ cause tremendous problems in an accurate determination of the reversal potential. Nevertheless, positive evidence that the reversal potential is located within the subthreshold range, covering the range reported here, has been reported *in vivo*⁸⁷ and *in vitro* in the acute slice

Table 4. Spiking activity of striatal secondary type II neurons (intracellular and extracellular recordings)

	Intracellular	n	Extracellular	n
Age (days)	23 ± 3	8	26 ± 3	6
Fmax† (spikes/s)*	5.4 ± 1.9	8	3.8 ± 1.1	6
INTH‡ 1p (ms)*	8.8 ± 2.8	8	6.6 ± 0.5	6
INTH‡ 2p (ms)*	156 ± 49	5	167 ± 64	6
Δt§ (ms)*	177 ± 54	7	140 ± 51	5
PSTH exc (ms)	—	—	16 ± 0.3	2
PSTH inh¶ (ms)	—	—	260 ± 10	2
PSTH reb** (ms)	—	—	290 ± 26	2

*Not different at $P < 0.05$; two-tailed Wilcoxon's rank sum test.

†Maximum firing rate, calculated using a sliding integration window (integration width: 3 s) and taking peak value.

‡Interval at first (1p) or second peak (2p) in the spike interval histogram.

§Duration of depression in spike discharge, which persists for several tens of milliseconds after the early peak in the AC. Time was taken from intersection with the base line in the AC.

||Time from cortical stimulation to the early peak in poststimulus time histogram (PSTH).

¶Time from early peak in poststimulus time histogram to the end of discharge inhibition.

**Time from cortical stimulation to maximum discharge peak in post-stimulus time histogram following the period of discharge inhibition.

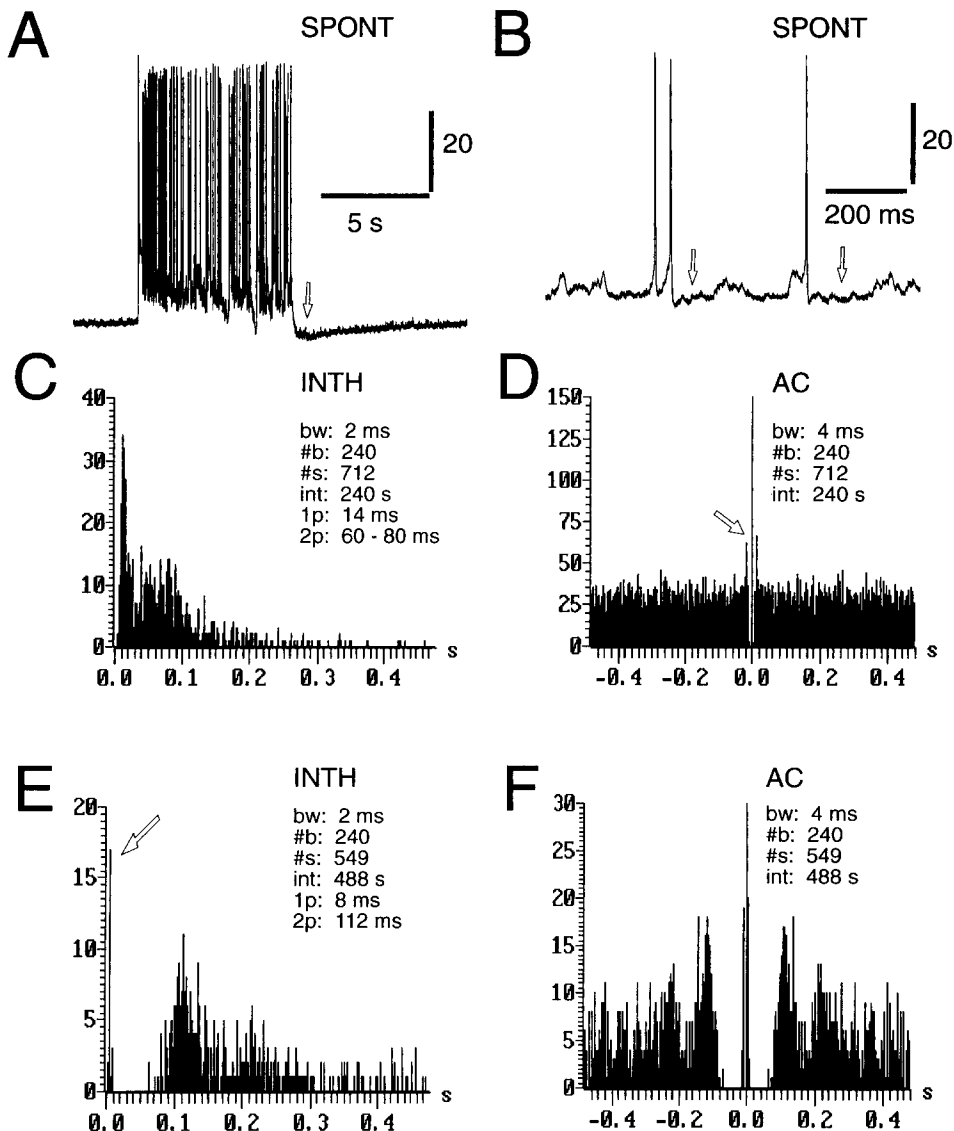


Fig. 18. Spontaneous activity in striatal secondary type II neurons. (A) Period of high activity followed by prominent AHP (arrow). (B) Most spikes show a prominent AHP (arrow). (C) The double-peaked distribution in the spike interval histogram reveals a clear predominance of short spike intervals around 14 ms and more widely distributed intervals in the range of 60–80 ms. (D) The flat AC, besides having an early narrow peak at 14 ms (arrow), shows no strong depression in spiking probability. Double-peaked spike interval histogram (E) and AC (F) of another secondary type II neuron show strong spike depression during the first 70 ms and strong oscillatory behavior (extracellular recording). A very narrow first peak at 7 ms (arrow) and a second peak at 112 ms are visible.

preparation.^{60,90} This leads to the conclusion that strong inhibition does not interrupt the “enabled” state in principal neurons, which is further supported by the absence of strong hyperpolarizing GABA_B-mediated inhibition.²³ As the membrane potential closely approaches the reversal potential of GABA_A activity, inhibition mainly acts via a shunting operation, which is a short-lasting, non-linear synaptic interaction. Thus, it seems fair to conclude that, if the shunting operation is a predominant feature in striatal group discharge, a precise timing among the spike activities of striatal neurons should be expected.¹⁰⁴

Stabilization of the “enabled” state by cholinergic activity

Early intracellular recordings *in vivo* have shown iontophoretically applied acetylcholine to have a slow, depolarizing effect in relatively depolarized striatal neurons. This slow depolarization could be antagonized by atropine.^{13,86} Extracellular recordings *in vivo* revealed similar slow time courses of excitation in striatal unit activity.¹⁶ Again, this effect was activity dependent, and was only observed in spontaneously active units. Intracellular recordings in slices under the presence of the muscarinic antagonist carbachol showed long-lasting depolarization upon

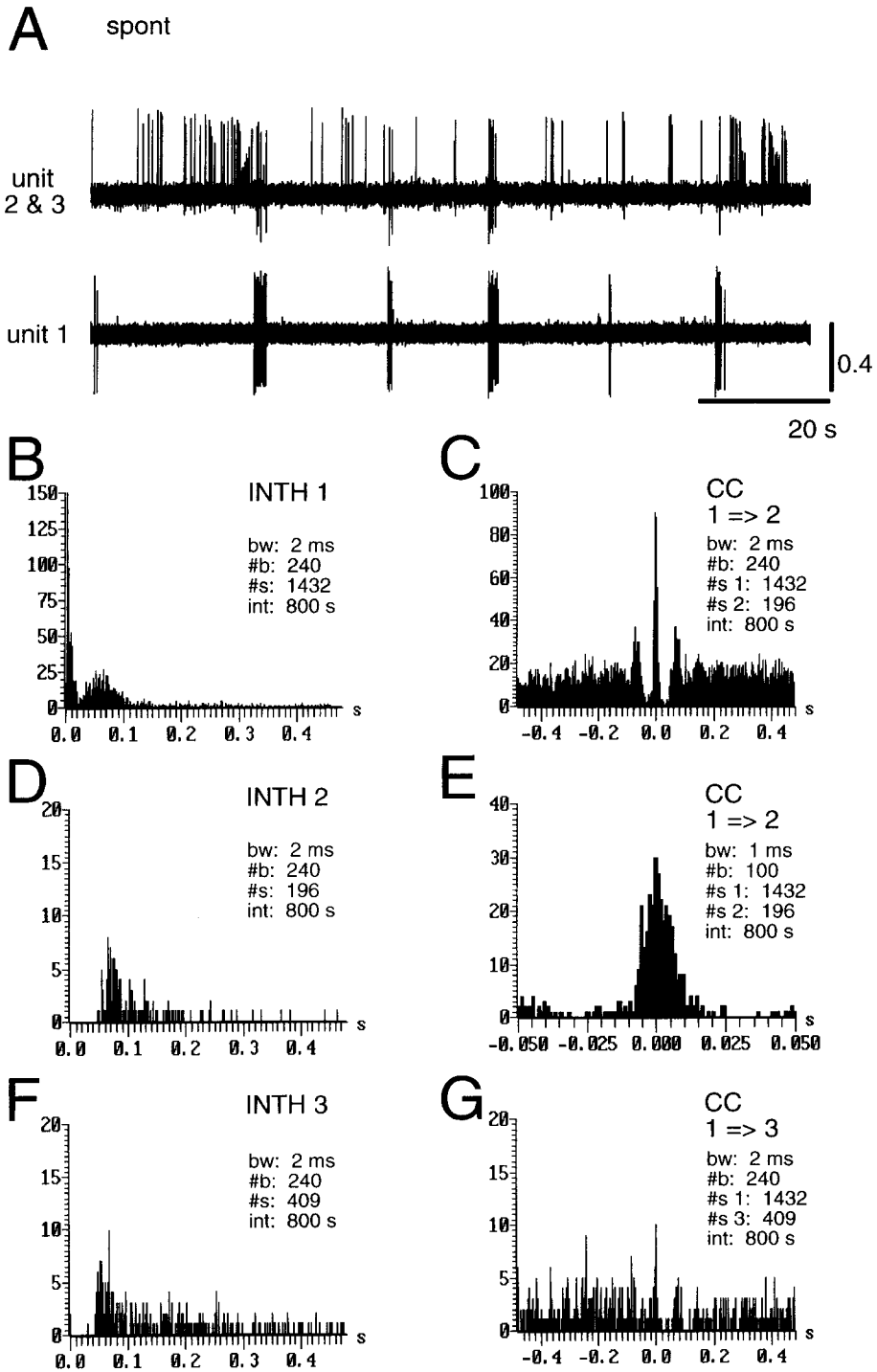


Fig. 19. Secondary type I neurons are involved in strong synchronized striatal discharge activity. CC between three simultaneously recorded striatal units. (A) Spontaneous activity of unit 1 (lower trace) and units 2 and 3 (upper trace), sampled on two different electrodes (0.9 mm apart). The time course in the lower trace shows biphasic spikes of single unit 1; the upper trace shows multi-unit activity, composed of biphasic unit 2 and mainly monophasic unit 3. The dot display above the time courses shows unit 1 (bottom), unit 2 (middle) and unit 3 (top). (B) The double-peaked spike interval histogram of unit 1. (C) CC between units 1 and 2 shows a synchronous oscillatory activity, with a central peak and two symmetric side peaks. (D) The single-peaked spike interval histogram of unit 2. (E) At high resolution the CC between units 1 and 2 clearly reveals the tight synchronization in spiking. (F) The single-peaked spike interval histogram of unit 3. (G) CC between units 1 and 3 does not indicate a strong correlation in firing. Note, however, the distinct timing relationships between the onsets and offsets of spiking between these units in the traces and the dot display in A.

pronounced intrastriatal stimulation due to the closure of a potassium channel.³⁹ Similar to our findings in the co-culture system, this particular muscarinic action on to neostriatal cells was not observed when the cells were at rest, where the membrane conductance is dominated by the anomalous rectifier.^{39,60,136} A muscarinic modulation of an A-current in striatal neurons was also proposed as having a stabilizing effect on the neurons' membrane potential.¹

At present, we cannot decide which currents dominate in the phenomena observed. Nevertheless, it was evident that principal neurons, once they became depolarized, were stabilized in the current membrane potential range by the action of acetylcholine on muscarinic receptors.

Secondary type I neurons

Secondary type I neurons are likely to represent the striatal GABAergic interneuron class (see companion paper). Most features of type I neurons are corroborated by several reports on striatal unit activity in rats. In immobilized, awake rats a few occurrences (two of 73) of stereotyped high-frequency bursting neurons, leading to AC as we described, have been reported.⁴⁷ Neurons, considered to be striatal GABAergic interneurons, responded to cortical stimulation with a short-lasting, high-frequency burst.¹¹² In the study of Williams and Millar,¹³⁵ neurons with a high discharge rate were also considered to be GABAergic interneurons. Kita, in a recent review,⁶⁹ described an aspiny neuron with a morphology similar to strong parvalbumin-positive cells, i.e. GABAergic interneurons, that responded to sensory-motor cortex stimulation with strong bursts.

We attribute the two different, but stereotyped ACs to different excitation levels. We showed that intracellular current injection at the cell body leads to a change in firing patterns. Low currents elicited a pure burst, whereas higher current injections led to single spikes followed by membrane potential rectification and discharge cessation. Various combinations of these two discharge behaviors lead to the two types of AC observed.

Oscillatory activity in the co-cultures and the role of inhibition

Secondary type I neurons, considered to be GABAergic interneurons, were the only striatal cell class that readily revealed 7–15 Hz oscillations. Their correlations with other striatal units over long distances suggest that the oscillations arise from common cortical inputs.³⁴ In addition, the oscillatory activity in type I neurons might originate from the striatal network itself, with the axonal arborizations of these neurons (Figs 3 and 14 in Ref. 104a), providing the anatomical basis for such long distance interactions. Indeed, the amount of inhibition present (Fig. 17E), the firing in strong bursts shown here and the strong connectivity among these neurons^{18,71}

should lead to an oscillatory response upon strong excitation.⁵

Secondary type II neurons

Non-bursting neurons with firing rates of two to seven spikes per second have been described in the rat¹⁴⁰ and alert monkey,^{3,64} and most likely correspond to cholinergic interneurons.⁸ Intracellular recordings *in vivo* support the view that the firing patterns of those neurons closely follow synaptic input.¹⁴⁰ Type II neurons in the co-cultures had firing patterns which most closely resembled those of cortical neurons. This indicates that, as was shown *in vivo*, the time structure of their synaptic input might be directly transferred into the corresponding spiking pattern. Anatomical studies have shown that cholinergic interneurons in the nucleus accumbens⁸⁸ and the caudate–putamen⁷⁶ receive mainly thalamic inputs. Nevertheless, in slices with corticostriatal projection fibers preserved, striatal interneurons with an electrophysiology resembling that of cholinergic interneurons are excited by white matter stimulation.⁶⁰ Hence, the spontaneous activity of type II neurons and the presence of cholinergic activity in the co-culture system support the view that cholinergic interneurons receive at least some cortical inputs.

Optophysiology

Spatial characteristics of neural activity. In view of the slow time course of glia signals⁵⁰ and the reduction of glia due to mitosis inhibitors during culturing, a large contribution of glia signals to the relative fluorescence change is very unlikely. Hence, the fluorescence signals we measured represent the spatiotemporal distribution of neuronal activity in the co-culture system. The fluorescence maps mainly reflect postsynaptic dendritic depolarizations since, unlike for example the hippocampus, the cortical and striatal networks lack a preferred internal orientation as well as a spatial segregation of cell bodies, axonal and dendritic processes.^{49,50,103} The optophysiological results demonstrated that neuronal activity spread in the co-culture in a characteristic spatiotemporal pattern with cortical excitation leading to a final overall depolarization in the striatum. This observation confirms findings using double-intracellular recordings *in vivo* that single auditory or somatosensory stimuli result in synchronized excitation of striatal regions several millimeters apart.¹⁴³

Although our results were obtained with local cortical microstimulation, it is likely that a similar activity pattern also develops upon local spontaneous cortical activity. Firstly, the time course of cortical fluorescence changes during spontaneously occurring activity were reflected with regard to build-up and stable net depolarization in the striatum. Secondly, simultaneously monitored extracellular spiking activity during optical recordings showed similar time courses to spontaneous intracellular and extracellular activity (see below). Thus, it is reasonable to assume

that a spontaneous volley of cortical activity leads to a similar spatially extended activation of the striatal network, as was shown here for the response to cortical microstimulation.

Temporal characteristics of neural activity. Upon cortical microstimulation all cell types in the co-culture system showed a typical sequence of early excitation, subsequent spike depression and long-lasting rebound excitation. This sequence was also often observed during spontaneous activity (see Figs 9 and 14). Similar sequences of cortical activity have been demonstrated in the anesthetized rat in layer V projection cells upon stimulation.^{34,75} Poststimulus time histograms from somatosensory cortex upon cutaneous and whisker stimulation^{30,119} or locomotion³² showed similar early excitations followed by various combinations of excitatory–inhibitory sequences, depending on movement state and anesthetics used.

Striatal responses *in vivo* also exhibit this sequence of early excitation, subsequent spike depression and long-lasting rebound excitation, as seen in the co-cultures. In cats, cortical stimulation induces an early peak excitation or a single-spike discharge after 17–21 ms.^{73,81,113} Early peak excitation values for the rat were in a similar range^{24,130} with the underlying polysynaptic postsynaptic potential arising mainly from the cortex.^{138,139} The subsequent spike depression *in vivo* ranged from 100 to 350 ms in the cat and the rat, and was followed by a long-lasting rebound excitation (for review see Wilson *et al.*¹³⁹). From the similarity to and the dependence on cortical activity, it was concluded that the general time course of early excitation, spike depression and subsequent

late excitation in the striatum mainly reflected the temporal properties of cortical activity patterns, rather than the dynamics of local striatal circuits.^{34,137} Our results from the co-culture system support this general view. However, this simple schematic picture of the “impulse response” of the cortical network to a synchronized synaptic volley and the subsequent responses of the striatal network did not cover the complete range of spontaneous activity dynamics seen in the co-culture. This was particularly evident when looking at multi-neuron activity in the co-culture system (Fig. 19).

CONCLUSIONS

Striatal activity is composed of a variety of different activity patterns, ranging from silent periods interrupted by selectively synchronized burst discharges to long-lasting excitation with sudden increases in firing, each of which can be temporally related to the other. The mechanisms underlying these intricate spatiotemporal dynamics and their relation to corticostriatal processing are still incompletely resolved. The organotypic cortex–striatum co-culture system will provide a powerful new *in vitro* approach for further research in that direction.

Acknowledgements—We thank Volker Staiger for skillful technical assistance, Amiram Grinvald for kindly providing us with the voltage-sensitive dye RH237, and Valentino Braitenberg and Jeff Wickens for inspiring discussions. One of the authors also wishes to thank Jeff Wickens for the kind hospitality in Dunedin while writing this manuscript. Additional support was received from the German “Bundesministerium für Forschung und Technologie” (BMFT).

REFERENCES

1. Akens P. T., Surmeier D. J. and Kitai S. T. (1990) Muscarinic modulation of a transient K⁺ conductance in rat neostriatal neurons. *Nature* **344**, 240–242.
2. Aldridge J. W. and Gilman S. (1991) The temporal structure of spike trains in the primate basal ganglia: afferent regulation of bursting demonstrated with precentral cerebral cortical ablation. *Brain Res.* **543**, 123–138.
3. Alexander G. E. and DeLong M. R. (1985) Microstimulation of the primate neostriatum. II. Somatotopic organization of striatal microexcitable zones and their relation to neuronal response properties. *J. Neurophysiol.* **53**, 1417–1430.
4. Alexander M. E. and Wickens J. R. (1993) Analysis of striatal dynamics: the existence of two modes of behavior. *J. theor. Biol.* **163**, 413–438.
5. Amari S. (1974) Mathematical theory of nerve nets. *Adv. Biophys., Tokyo* **6**, 75–119.
6. Andersen P. and Eccles S. J. (1962) Inhibitory phasing of neuronal discharge. *Nature* **196**, 645–647.
7. Anderson J. E. (1977) Discharge patterns of basal ganglia neurons during active maintenance of postural stability and adjustment to chair tilt. *Brain Res.* **143**, 325–338.
8. Aosaki T., Kimura M. and Graybiel A. M. (1992) Physiologically identified tonically active neurons of primate striatum lie in the matrix compartment. *IBAGS IV, Fourth Triennial Meeting of the International Basal Ganglia Society* 3 (Abstract).
9. Apicella P., Scarnati E. and Schultz W. (1991) Tonically discharging neurons of monkey striatum respond to preparatory and rewarding stimuli. *Expl Brain Res.* **84**, 672–675.
10. Armstrong-James M. and Fox K. (1988) Evidence for a specific role for cortical NMDA receptors in slow-wave sleep. *Brain Res.* **451**, 189–196.
11. Baldino F., Wolfson B., Heinemann U. and Gutnick M. J. (1986) An N-methyl-D-aspartate (NMDA) receptor antagonist reduces bicuculline-induced depolarization shifts in neocortical explant cultures. *Neurosci. Lett.* **70**, 101–105.
12. Bargas J., Galarraga E. and Aceves J. (1989) An early outward conductance modulates the firing latency and frequency of neostriatal neurons of the rat brain. *Expl Brain Res.* **75**, 146–156.
13. Bernardi G., Floris V., Marciani M. G., Morocutti C. and Stanzione P. (1976) The action of acetylcholine and L-glutamic acid on rat caudate neurons. *Brain Res.* **114**, 134–138.

14. Bingmann D., Speckmann E.-J., Baker R. E., Ruikter J. and de Jong B. M. (1988) Differential antiepileptic effects of the organic calcium antagonists verapamil and flunarizine in neurons of organotypic neocortical explants. *Expl Brain Res.* **72**, 439–442.
15. Bishop G. A., Chang H. T. and Kitai S. T. (1982) Morphological and physiological properties of neostriatal neurons: an intracellular horseradish peroxidase study in the rat. *Neuroscience* **7**, 179–191.
16. Bloom F. E., Costa E. and Salmoiraghi G. C. (1965) Anesthesia and the responsiveness of individual neurons of the caudate nucleus of the cat to acetylcholine, norepinephrine and dopamine administered by microelectrophoresis. *J. Pharmac. exp. Ther.* **150**, 244–252.
17. Bolam J. P. and Izzo P. N. (1988) The postsynaptic targets of substance P immunoreactive terminals in the rat neostriatum with particular reference to identified spiny striatonigral neurons. *Expl Brain Res.* **70**, 361–377.
18. Bolam J. P., Powell J. F., Wu J.-Y. and Smith A. D. (1985) Glutamate decarboxylase-immunoreactive structures in the rat neostriatum: a correlated light and electron microscopic study including a combination of Golgi-impregnation with immunocytochemistry. *J. comp. Neurol.* **237**, 1–20.
19. Bonhoeffer T. and Staiger V. (1988) Optical recording with single cell resolution from monolayered slice cultures of rat hippocampus. *Neurosci. Lett.* **92**, 259–264.
20. Buser P., Pouderoux G. and Mereaux J. (1974) Single-unit recording in the caudate nucleus during sessions with elaborate movements in the awake monkey. *Brain Res.* **71**, 337–344.
21. Cajal S. R. (1911) *Histologie du Système Nerveux*. A. Maloine, Paris.
22. Cajal S. R. (1959) *Degeneration and Regeneration of the Nervous System*. Hafner, New York.
23. Calabresi P., Mercuri N. B., De Murtas M. and Bernardi G. (1991) Involvement of GABA systems in feedback regulation of glutamate- and GABA-mediated synaptic potentials in rat neostriatum. *J. Physiol., Lond.* **440**, 581–599.
24. Calabresi P., Mercuri N. B., Stefani A. and Bernardi G. (1990) Synaptic and intrinsic control of membrane excitability of neostriatal neurons. I. An *in vivo* analysis. *J. Neurophysiol.* **63**, 651–662.
25. Calabresi P., Misgeld U. and Dodt H.-U. (1987) Intrinsic membrane properties of neostriatal neurons can account for their low level of spontaneous activity. *Neuroscience* **20**, 293–303.
26. Calvet M.-C. (1974) Patterns of spontaneous electrical activity in tissue cultures of mammalian cerebral cortex vs. cerebellum. *Brain Res.* **69**, 281–295.
27. Cäsler M., Bonhoeffer T. and Bolz J. (1989) Cellular organization and development of slice cultures from rat visual cortex. *Expl Brain Res.* **477**, 234–244.
28. Chang H. T. and Kita H. (1992) Interneurons in the rat striatum: relationships between parvalbumin neurons and cholinergic neurons. *Brain Res.* **574**, 307–311.
29. Chang H. T., Wilson C. J. and Kitai S. T. (1981) Single neostriatal efferent axons in the globus pallidus: a light and electron microscopic study. *Science* **213**, 915–918.
30. Chapin J. K., Waterhouse B. D. and Woodward D. J. (1981) Differences in cutaneous sensory response properties of single somatosensory cortical neurons in awake and halothane anesthetized rats. *Brain Res. Bull.* **6**, 63–70.
31. Cherubini E., Rovira C., Gaiarsa J. L., Corradetti R. and Ben-Ari Y. (1990) GABA mediated excitation in immature rat CA3 hippocampal neurons. *Int. J. devl Neurosci.* **8**, 481–490.
32. Chin C. and Chapin J. K. (1990) Movement induced modulation of afferent transmission to single neurons in the ventroposterior thalamus and somatosensory cortex in rat. *Brain Res.* **81**, 515–522.
33. Cohen L. B. and Salzberg B. M. (1978) Optical methods for monitoring neuron activity. *A. Rev. Neurosci.* **1**, 171–182.
34. Cowan R. L. and Wilson C. J. (1994) Spontaneous firing patterns and axonal projections of single cortico-striatal neurons in the rat medial agranular cortex. *J. Neurophysiol.* **71**, 17–32.
35. Crain S. M. (1966) Development of ‘organotypic’ bioelectric activity in central nervous tissues during maturation in culture. *Int. Rev. Neurobiol.* **9**, 1–43.
36. Crain S. M. and Bornstein M. B. (1964) Bioelectric activity of neonatal mouse cerebral cortex during growth and differentiation in tissue culture. *Expl Neurol.* **10**, 425–450.
37. Creutzfeld O. D. and Houchin J. (1974) Neuronal basis of EEG waves. In *Handbook of Electroencephalography and Clinical Neurophysiology* (ed. Creutzfeld O. D.), Vol. 2, Part C, pp. 5–55. Elsevier, Amsterdam.
38. Crutcher M. D. and DeLong M. R. (1984) Single cell studies of the primate putamen. I. Functional organization. *Expl Brain Res.* **53**, 233–243.
39. Dodt H.-U. and Misgeld U. (1986) Muscarinic slow excitation and muscarinic inhibition of synaptic transmission in the rat neostriatum. *J. Physiol., Lond.* **380**, 593–608.
40. Echlin F. A. (1959) The supersensitivity of chronically ‘isolated’ cerebral cortex as a mechanism in focal epilepsy. *Electroenceph. clin. Neurophysiol.* **11**, 697–722.
41. Eeckman F. H. and Freeman W. J. (1991) Asymmetric sigmoid non-linearity in the rat olfactory system. *Brain Res.* **557**, 13–21.
42. Erb M. and Aertsen A. (1992) Dynamics of activity in biology-oriented neural network models: stability at low firing rates. In *Information Processing in the Cortex: Experiments and Theory* (eds Aertsen A. and Braitenberg V.), pp. 201–224. Springer, Berlin.
43. Fox K. and Armstrong-James M. (1986) The role of the anterior intralaminar nuclei and *N*-methyl-D-aspartate receptors in the generation of spontaneous bursts in rat neocortical neurons. *Expl Brain Res.* **63**, 505–518.
44. Gähwiler B. H. (1981) Organotypic monolayer cultures of nervous tissue. *J. Neurosci. Meth.* **4**, 329–342.
45. Gähwiler B. H. (1989) Organotypic cultures of neural tissue. *Trends Neurosci.* **11**, 484–489.
46. Gardiner T. W. and Kitai S. T. (1992) Single-unit activity in the globus pallidus and neostriatum of the rat during performance of a trained head movement. *Expl Brain Res.* **88**, 517–530.
47. Godukhin O. V. (1981) Types of spiking activity and nature of neuronal interrelations in the rat neostriatum. *Neirofiziologia* **13**, 571–579.
48. Götz M. and Bolz J. (1992) Formation and preservation of cortical layers in slice cultures. *J. Neurobiol.* **23**, 783–802.
49. Grinvald A. (1985) Real-time optical mapping of neuronal activity: from single growth cones to the intact mammalian brain. *A. Rev. Neurosci.* **8**, 263–305.
50. Grinvald A., Frostig R. D., Lieke E. and Hildesheim R. (1988) Optical imaging of neuronal activity. *Physiol. Rev.* **68**, 1285–1366.

51. Gutnick M. J., Connors B. W. and Prince D. A. (1982) Mechanism of neocortical epileptogenesis *in vitro*. *J. Neurophysiol.* **48**, 1321–1335.
52. Gutnick M. J., Wolfson B. and Baldino F. (1989) Synchronized neuronal activities in neocortical explant cultures. *Expl Brain Res.* **76**, 131–140.
53. Habets A. M. M., Van Dongen A. M. J., Van Huizen F. and Corner M. A. (1987) Spontaneous neuronal firing patterns in fetal rat cortical networks during development *in vitro*: a quantitative analysis. *Expl Brain Res.* **69**, 43–52.
54. Hablitz J. J. (1987) Spontaneous ictal-like discharges and sustained potential shifts in the developing rat neocortex. *J. Neurophysiol.* **58**, 1052–1065.
55. Hall R. D. and Lindholm E. P. (1974) Organization of motor and somatosensory neocortex in the albino rat. *Brain Res.* **73**, 249–255.
56. Hikosaka O., Sakamoto M. and Usui S. (1989) Functional properties of monkey caudate neurons. I. Activities related to saccadic eye movements. *J. Neurophysiol.* **61**, 780–798.
57. Holmes O. and Houchin J. (1966) Units in the cerebral cortex of the anesthetized rat and the correlations between their discharges. *J. Physiol., Lond.* **187**, 651–671.
58. Jaeger D., Gilman S. and Aldridge J. W. (1993) Primate basal ganglia activity in a precued reaching task: preparation for movement. *Expl Brain Res.* **95**, 51–64.
59. Jaeger D., Kita H. and Wilson C. J. (1994) Surround inhibition among projection neurons is weak or nonexistent in the rat neostriatum. *J. Neurophysiol.* **72**, 2555–2558.
60. Jiang Z.-G. and North R. A. (1991) Membrane properties and synaptic responses of rat striatal neurones *in vitro*. *J. Physiol., Lond.* **443**, 533–553.
61. Katayama Y., Miyazaki S. and Tsubokawa T. (1981) Electrophysiological evidence favoring intracaudate axon collaterals of GABAergic caudate output neurons in the cat. *Brain Res.* **216**, 180–186.
62. Kawaguchi Y., Wilson C. J. and Emson P. (1989) Intracellular recording of identified neostriatal patch and matrix spiny cells in a slice preparation preserving cortical inputs. *J. Neurophysiol.* **62**, 1052–1068.
63. Kemp J. M. and Powell T. P. S. (1971) The structure of the caudate nucleus of the cat: light and electron microscopy. *Phil. Trans. R. Soc. Lond.* **262**, 383–401.
64. Kimura M. (1986) The role of primate putamen neurons in the association of sensory stimuli with movement. *Neurosci. Res.* **3**, 436–443.
65. Kimura M. (1990) Behaviorally contingent property of movement-related activity of the primate putamen. *J. Neurophysiol.* **63**, 1277–1296.
66. Kimura M., Aosaki T., Ishida A. and Watanabe K. (1992) Activity of primate putamen neurons is selective to the mode of voluntary movement: visually guided, self-initiated or memory guided. *Expl Brain Res.* **89**, 473–477.
67. Kimura M., Kato M. and Shimazaki H. (1990) Physiological properties of projection neurons in the monkey striatum to the globus pallidus. *Expl Brain Res.* **82**, 672–676.
68. Kimura M., Rajkowski J. and Everts E. V. (1984) Tonicly discharging putamen neurons exhibit set dependent responses. *Proc. natn. Acad. Sci. U.S.A.* **81**, 4998–5001.
69. Kita H. (1993) GABAergic circuits of the striatum. In *Chemical Signaling in the Basal Ganglia* (eds Arbuthnott G. W. and Emson P. C.), pp. 51–72. *Progress in Brain Research*, Vol. 99. Elsevier, Amsterdam.
70. Kita H., Kita T. and Kitai S. T. (1985) Regenerative potentials in rat neostriatal neurons in an *in vitro* slice preparation. *Expl Brain Res.* **60**, 63–70.
71. Kita H. and Kitai S. T. (1988) Glutamate decarboxylase immunoreactive neurons in rat neostriatum: their morphological types and populations. *Brain Res.* **447**, 346–352.
72. Kita H., Kosaka T. and Heizmann C. W. (1990) Parvalbumin-immunoreactive neurons in the rat neostriatum: a light and electron microscopic study. *Brain Res.* **536**, 1–15.
73. Kocsis J. D., Sugimori M. and Kitai S. T. (1977) Convergence of excitatory synaptic inputs to caudate spiny neurons. *Brain Res.* **124**, 403–413.
74. Kriegstein A. R., Suppes T. and Prince D. A. (1987) Cellular and synaptic physiology and epileptogenesis of developing rat neocortical neurons *in vitro*. *Devl Brain Res.* **34**, 161–171.
75. Landry P., Wilson C. J. and Kitai S. T. (1984) Morphological and electrophysiological characteristics of pyramidal tract neurons in the rat. *Expl Brain Res.* **57**, 177–190.
76. Lapper S. R. and Bolam J. P. (1992) Input from the frontal cortex and the parafascicular nucleus to cholinergic interneurons in the dorsal striatum of the rat. *Neuroscience* **51**, 533–545.
77. Lapper S. R., Smith Y., Sadikot A. F., Parent A. and Bolam J. P. (1992) Cortical input to parvalbumin-immunoreactive neurons in the putamen of the squirrel monkey. *Brain Res.* **580**, 215–224.
78. Lee W. and Hablitz J. J. (1991) Initiation of epileptiform activity by excitatory amino acid receptors in the disinhibited rat neocortex. *J. Neurophysiol.* **65**, 87–95.
79. Leiman A. L., Seil F. J. and Kelly M. J. III (1975) Maturation of electrical activity of cerebral neocortex in tissue culture. *Expl Neurol.* **48**, 275–291.
80. Lighthall J. W., Park M. R. and Kitai S. T. (1981) Inhibition in slices of rat neostriatum. *Brain Res.* **212**, 182–187.
81. Liles S. L. (1974) Single-unit responses of caudate neurons to stimulation of frontal cortex, substantia nigra and entopeduncular nucleus in cats. *J. Neurophysiol.* **37**, 254–265.
82. Lu E. J. and Brown W. J. (1977) The developing caudate nucleus in the euthyroid and hypothyroid rat. *J. comp. Neurol.* **171**, 261–284.
83. Luhmann H. J. and Prince D. A. (1991) Postnatal maturation of the GABAergic system in rat neocortex. *J. Neurophysiol.* **65**, 247–263.
84. Lytton W. W. and Sejnowski T. J. (1990) Simulations of cortical pyramidal neurons synchronized by inhibitory interneurons. *J. Neurophysiol.* **66**, 1059–1079.
85. McGeorge A. J. and Faull R. L. M. (1989) The organization of the projection from the cerebral cortex to the striatum in the rat. *Neuroscience* **29**, 503–537.
86. McLennan H. and York D. H. (1966) Cholinergic mechanism in the caudate nucleus. *J. Physiol., Lond.* **187**, 163–175.
87. Mercuri N. B., Calabresi P., Stefani A., Stratta F. and Bernardi G. (1991) GABA depolarizes neurons in the rat striatum: an *in vivo* study. *Synapse* **8**, 38–40.

88. Meredith G. E. and Wouterlood F. G. (1990) Hippocampal and midline thalamic fibers and terminals in relation to the choline acetyltransferase-immunoreactive neurons in nucleus accumbens of the rat: a light and electron microscopic study. *J. comp. Neurol.* **296**, 204–221.
89. Misgeld U., Frotscher M. and Wagner A. (1984) Identification of projecting neurons in rat neostriatal slices. *Brain Res.* **299**, 367–370.
90. Misgeld U., Wagner A. and Ohno T. (1982) Depolarizing IPSPs and depolarization by GABA of rat neostriatum cells *in vitro*. *Exptl Brain Res.* **45**, 108–114.
91. Morishita I. and Yajima A. (1972) Analysis and stimulation of networks of mutually inhibiting neurons. *Kybernetik* **11**, 154–165.
92. Neuman R. S. and Zebrowska G. (1992) Serotonin (5-HT₂) receptor mediated enhancement of cortical unit activity. *Can. J. Physiol. Pharmacol.* **70**, 1604–1609.
93. Niki H., Sakai M. and Kubota K. (1971) Delayed alternation performance and unit activity of the caudate head and medial orbito-frontal gyrus in the monkey. *Brain Res.* **38**, 343–353.
94. Nisenbaum E. S., Stricker E. M., Zigmond M. J. and Berger T. W. (1986) Long-term effects of dopamine-depleting brain lesions on spontaneous activity of Type II striatal neurons: relation to behavioral recovery. *Brain Res.* **398**, 221–230.
95. Nishino H., Hattori S., Muramoto K. and Ohno T. (1991) Basal ganglia neural activity during operant feeding behavior in the monkey: relation to sensory integration and motor execution. *Brain Res. Bull.* **27**, 463–468.
96. Noda H. and Adey W. R. (1970) Firing of neuron pairs in cat association cortex during sleep and wakefulness. *J. Neurophysiol.* **33**, 672–684.
97. Oertel W. H. and Mugnaini E. (1984) Immunocytochemical studies of GABAergic neurons in rat basal ganglia and their relationships to other neuronal systems. *Neurosci. Lett.* **47**, 233–238.
98. Park M. R., Lighthall J. W. and Kitai S. T. (1980) Recurrent inhibition in the rat neostriatum. *Brain Res.* **194**, 359–369.
99. Paxinos G. and Watson C. (1982) *The Rat Brain in Stereotaxic Coordinates*. Academic Press, Sydney.
100. Perkel D. H., Gerstein G. L. and Moore G. P. (1967) Neuronal spike trains and stochastic point processes. I. The single spike train. *Biophys. J.* **7**, 391–417.
101. Perkel D. H., Gerstein G. L. and Moore G. P. (1967) Neuronal spike trains and stochastic point processes. II. Simultaneous spike trains. *Biophys. J.* **7**, 419–440.
102. Pirch J. H. (1993) Basal forebrain and frontal-cortex neuron responses during visual-discrimination in the rat. *Brain Res. Bull.* **31**, 73–83.
103. Plenz D. and Aertsen A. (1993) Current source density profiles of optical recording maps: a new approach to the analysis of spatio-temporal neural activity patterns. *Eur. J. Neurosci.* **5**, 437–448.
104. Plenz D. and Aertsen A. (1994) The basal ganglia: ‘minimal coherence detection’ in cortical activity distributions. In *The Basal Ganglia. IV. New Ideas and Data on Structure and Function* (eds Percheron G., McKenzie J. S. and Feger J.), pp. 579–588. Plenum Press, New York.
- 104a. Plenz D. and Aertsen A. (1995) Neural dynamics in cortex–striatum co-cultures—I. Anatomy and electrophysiology of neuronal cell types. *Neuroscience* **70**, 861–891.
105. Preston R. J., Bishop G. A. and Kitai S. T. (1980) Medium spiny neuron projection from the rat striatum: an intracellular horseradish peroxidase study. *Brain Res.* **183**, 253–263.
106. Prince D. A. (1968) The depolarization shift in “epileptic” neurons. *Exptl Neurol.* **21**, 467–485.
107. Prince D. A. (1978) Neurophysiology of epilepsy. *A. Rev. Neurosci.* **1**, 395–415.
108. Purpura D. P. and Housepian E. M. (1961) Morphological and physiological properties of chronically isolated immature neocortex. *Exptl Neurol.* **4**, 377–401.
109. Qian N. and Sejnowski T. J. (1990) When is an inhibitory synapse effective? *Proc. natn. Acad. Sci. U.S.A.* **87**, 8145–8159.
110. Rebec G. V. and Curtis S. D. (1988) Reciprocal zones of excitation and inhibition in the neostriatum. *Synapse* **2**, 633–635.
111. Ribak C. E., Vaughn J. E. and Roberts E. (1979) The GABA neurons and their axon terminals in rat corpus striatum as demonstrated by GAD immunohistochemistry. *J. comp. Neurol.* **187**, 261–284.
112. Richardson T. L., Miller J. J. and McLennan H. (1977) Mechanisms of excitation and inhibition in the nigrostriatal system. *Brain Res.* **127**, 219–234.
113. Rocha-Miranda C. E. (1965) Single-unit analysis of cortex–caudate connections. *Electroenceph. clin. Neurophysiol.* **19**, 237–247.
114. Romijn H. J., Ruijter J. M. and Wolters P. S. (1988) Hypoxia preferentially destroys GABAergic neurons in the developing rat neocortex explants in culture. *Exptl Neurol.* **100**, 332–340.
115. Salzberg B. M. (1989) Optical recording of voltage changes in nerve terminals and in fine neuronal processes. *A. Rev. Physiol.* **51**, 507–526.
116. Schaer M. (1974) Decrease in ionized calcium by bicarbonate in physiological solutions. *Pflügers Arch.* **347**, 249–254.
117. Schultz W. and Romo R. (1988) Neuronal activity in the monkey striatum during the initiation of movements. *Exptl Brain Res.* **71**, 431–436.
118. Seite R., Vuillet-Luciani J., Vio M. and Cataldo C. (1977) Sur la présence d’inclusions nucléaires dans certain neurones du noyau caudé du rat: répartition, fréquence et organisation ultrastructurale. *Biol. Cell* **30**, 73–76.
119. Simons D. J., Carvell G. E., Hershey A. E. and Bryant D. P. (1992) Responses of barrel cortex neurons in awake rats and effects of urethane anesthesia. *Exptl Brain Res.* **91**, 259–272.
120. Somogyi P., Bolam J. P. and Smith A. D. (1981) Monosynaptic cortical input and local axon collaterals of identified striatonigral neurons. A light and electron microscopic study using the Golgi–peroxidase transport degeneration procedure. *J. comp. Neurol.* **195**, 567–584.
121. Steriade M., Gloor P., Llinás R., Lopes da Silva F. H. and Mesulam M.-M. (1990) Basic mechanism of cerebral rhythmic activities. *Electroenceph. clin. Neurophysiol.* **76**, 481–508.
122. Sugimori M., Preston R. J. and Kitai S. T. (1978) Response properties and electrical constants of caudate nucleus neurons in the cat. *J. Neurophysiol.* **41**, 1662–1676.
123. Surmeier D. J., Eberwine J., Wilson C. J., Cao Y., Stefani A. and Kitai S. T. (1992) Dopamine receptor colocalize in rat striatonigral neurons. *Proc. natn. Acad. Sci. U.S.A.* **89**, 10178–10182.

124. Surmeier D. J. and Kitai S. T. (1993) D1 and D2 dopamine receptor modulation of sodium and potassium currents in rat neostriatal neurons. In *Chemical Signaling in the Basal Ganglia* (eds Arbuthnott G. W. and Emson P. C.), pp. 309–324. Elsevier, Amsterdam.
125. Surmeier D. J., Stefani A., Foehring R. C. and Kitai S. T. (1991) Developmental regulation of a slowly-inactivating potassium conductance in rat neostriatal neurons. *Neurosci. Lett.* **122**, 41–46.
126. Thompson S. M., Deisz R. A. and Prince D. A. (1988) Relative contributions of passive equilibrium and active transport to the distribution of chloride in mammalian cortical neurons. *J. Neurophysiol.* **60**, 105–124.
127. Thompson S. M. and Gähwiler B. H. (1989) Activity-dependent disinhibition. II. Effects of extracellular potassium, Furosemide, and membrane potential on ECL in hippocampal CA3 neurons. *J. Neurophysiol.* **61**, 512–523.
128. Thompson S. M. and Gähwiler B. H. (1989) Activity-dependent disinhibition. I. Repetitive stimulation reduces IPSP driving force and conductance in the hippocampus *in vitro*. *J. Neurophysiol.* **61**, 501–511.
129. Tschanz J. T., Haracz J. L., Griffith K. E. and Rebec G. V. (1991) Bilateral cortical ablations attenuate amphetamine-induced excitations of neostriatal motor-related neurons in freely moving rats. *Neurosci. Lett.* **134**, 127–130.
130. Vandermaelen C. P. and Kitai S. T. (1981) Intracellular analysis of synaptic potentials in rat neostriatum following stimulation of the cerebral cortex, thalamus and substantia nigra. *Brain Res. Bull.* **5**, 725–733.
131. Welker C. (1971) Microelectrode delineation of fine grain somatotopic organization of Sml cerebral neocortex in albino rat. *Brain Res.* **26**, 259–275.
132. West M. O., Carelli R. M., Pomerantz M., Cohen S. M., Gardner J. P., Chapin J. K. and Woodward D. J. (1990) A region in the dorsolateral striatum of the rat exhibiting single-unit correlations with specific locomotor limb movements. *J. Neurophysiol.* **64**, 1233–1244.
133. Wickens J. R., Alexander M. E. and Miller R. (1991) Two dynamic modes of striatal function under dopaminergic-cholinergic control: simulation and analysis of a model. *Synapse* **8**, 1–12.
134. Wickens J. R. and Arbuthnott G. W. (1993) The cortico-striatal system on computer simulation: an intermediate mechanism for sequencing actions. In *Chemical Signaling in the Basal Ganglia* (eds Arbuthnott G. W. and Emson P. C.), pp. 325–340. *Progress in Brain Research*, Vol. 99. Elsevier, Amsterdam.
135. Williams G. V. and Millar J. (1990) Concentration-dependent actions of simulated dopamine release on neuronal activity. *Neuroscience* **39**, 1–16.
136. Wilson C. J. (1992) Dendritic morphology, inward rectification and the functional properties of neostriatal neurons. In *Single Neuron Computation* (eds McKenna T., Davis J. and Zornetzer S. F.), pp. 141–171. Academic Press, San Diego.
137. Wilson C. J. (1993) The generation of natural firing patterns in neostriatal neurons. In *Chemical Signaling in the Basal Ganglia* (eds Arbuthnott G. W. and Emson P. C.), pp. 277–298. *Progress in Brain Research*, Vol. 99. Elsevier, Amsterdam.
138. Wilson C. J., Chang H. T. and Kitai S. T. (1983) Origins of post synaptic potentials evoked in spiny neostriatal projection neurons by thalamic stimulation in the rat. *Expl Brain Res.* **51**, 217–226.
139. Wilson C. J., Chang H. T. and Kitai S. T. (1983) Disfacilitation and long-lasting inhibition of neostriatal neurons in the rat. *Expl Brain Res.* **51**, 227–235.
140. Wilson C. J., Chang H. T. and Kitai S. T. (1990) Firing patterns and synaptic potentials of identified giant aspiny interneurons in the rat neostriatum. *J. Neurosci.* **10**, 508–519.
141. Wilson C. J. and Groves P. M. (1980) Fine structure and synaptic connections of the common spiny neuron of the rat neostriatum: a study employing intracellular injection of horseradish peroxidase. *J. comp. Neurol.* **194**, 599–615.
142. Wilson C. J. and Groves P. M. (1981) Spontaneous firing patterns of identified spiny neurons in the rat neostriatum. *Brain Res.* **220**, 67–80.
143. Wilson J. S., Hull C. D. and Buchwald N. A. (1983) Intracellular studies of the convergence of sensory input on caudate neurons of the cat. *Brain Res.* **270**, 197–208.
144. Wolfson B., Gutnick M. J. and Baldino F. (1989) Electrophysiological characteristics of neurons in neocortical explant cultures. *Expl Brain Res.* **76**, 122–130.

(Accepted 28 July 1995)